University Mohamed Khider de Biskra
Faculty of Exact Sciences and Sciences of Nature and Life
Matter Sciences Department

Dissertation of Master

Filed of Matter Sciences
Physics
Physics of Energies and Renewable Energies

Ref. :

Presented by :
Zerarka Selssabil
Seridji Baya

The :

Study of electron transport effect on perovskite solar cells using simulation

---

Jury :

Ouahab Abdelouahab	Professor	Mehamaed University -Biskra	President
Boumaraf Rami	M.C.B	Mehamaed University -Biskra	Supervisor
Boudib Ouahiba	M.A.A	Mehamaed University -Biskra	Examiner

Academic year : 2019/2020

Dedication

This dissertation is dedicated to our family who supported us.

To the best mothers "Karima", "Djamila"

To the best fathers "Madjid"

To the brother "Mohamed salah"

To the sister "Kaouthar"

Acknowledgement

First and the foremost, we thankful to “ALLAH”, for to give us an opportunity, determination, and strength to complete this research work, despite the existence of some challenges as the first extensive experience and under the pressure of the epidemic, but this did not prevent it for being a wonderful experiment in the field of scientific research of simulation solar cell.

We would like to thank Dr.Boumaraf Rami for supervising us and for his efforts in assisting us with this work, despite the problem of personal communication due to the epidemic that has swept the world, and his attempt to explain in the smallest detail the work.

We are grateful to our family for supporting us during this period of research, so we can achieve our goals without their cooperation and affection.

In the end, we would also like to thank all of our friends, with whom we had many experiences and memories.

ملخص

تلعب طبقة نقل الإلكترونات (ETL) دورا مهما في استخراج ونقل الإلكترونات المتولدة ضوئيًا. لتحديد تأثيرها على سلوك وأداء الخلايا الشمسية بيروفسكايت. قمنا بدراسة تأثير طبقة نقل الإلكترون (ETL) باستخدام برنامج المحاكاة (SCAPS-1D)، حيث استعمل لمحاكاة تأثير معلمات فيزيائية مختلفة مثل السمك وتركيز التطعيم، وكثافة العيوب وكثافة العيوب الأسطح البينية لـ ETM / Perovskite على الخصائص الكهربائية للخلية الشمسية (كثافة تيار الدارة القصيرة الحالية (Jsc)، وجهد الدائرة المفتوحة (Voc)، معامل التعبئة (FF)، وكفاءة تحويل الطاقة (PCE))، باستخدام TiO_2 وZnO كنوعين من مواد نقل الإلكترونات (ETM). يجدر الإشارة إلى أن زيادة السمك تركيز التطعيم وكثافة العيوب وكثافة العيوب الأسطح البينة ETM / Perovskite يمكن أن تلعب دورا مهما في أداء الخلايا الشمسية. وفي الأخير، تمت مقارنة أداء المواد المستعملة في طبقة نقل الإلكترون (ETL) حيث وجدنا أن مادة TiO_2 أفضل أداء من مادة ZnO كطبقة نقل إلكترونات.

Abstract

The electron transport layer (ETL) plays a vital role in extracting and transporting photogenerated electrons. To determine their impact on perovskite solar cell behaviour and performance, we have studied the effect of electron transport layer (ETL) using simulation program (SCAPS-1D). A simulation is carried out to study the effect of different physical parameters such as thickness, doping concentration, defect density and interface trap density of ETM/Perovskite on the electrical properties of a solar cell (the short-circuit current density (Jsc), open-circuit voltage (Voc), fill factor (FF), and power conversion efficiency (PCE)), using TiO_2 and ZnO as two types of electron transport material (ETM). It is also indicated that an increase in the thickness, donor concentration, defect density and interface trap density of ETL/Perovskite may have a great effect on the performance of solar cells. Another important result of this study is TiO_2 has better conversion performance than ZnO material as electron transport layer.

Résumé

La couche de transport d'électrons (ETL) joue un rôle vital dans l'extraction et le transport d'électrons photogénérés. Pour déterminer leur impact sur le comportement et les performances des cellules solaires perovskites, nous avons étudié l'effet de la couche de transport d'électrons (ETL) à l'aide d'un programme de simulation (SCAPS-1D) pour simuler l'effet de différents paramètres physiques tels que l'épaisseur et la concentration de dopage, la densité des défauts et la densité des défauts d'interface de l'ETM/Perovskite sur les propriétés électriques d'une cellule solaire (densité de courant de court-circuit (Jcs), tension en circuit ouvert (Vco), facteur de remplissage (FF) et efficacité de conversion d'énergie (PCE)), utilisant TiO2 et ZnO comme deux types de matériel de transport d'électrons (ETM). Il est également indiqué qu'une augmentation de l'épaisseur ou la concentration des donneurs, de la densité des défauts et de la densité des pièges d'interface de l'ETL/Perovskite peut affecter la performance des cellules solaires. Un autre résultat important de cette étude est que le matériau TiO2 a de meilleures performances de conversion que le matériau ZnO comme couche de transport d'électrons.

Table of Contents

List of Figures

List of Tables

List of Symbols

SCAPS	Solar Cell Capacitance Simulator
PV	Photovoltaic
AM 1.5	Standard terrestrial solar spectrum ‘Air Mass 1.5’
λ	Wavelength
I	Total current
I_0	Saturation current
I_L	Light generated current
q	Electronic charge
V	Applied potential
η	Ideality factor
K	Boltzmann’s constant
T	Environment temperature
H	Planck’s constant
C	Light speed
J-V	Current-density vs. voltage
Jsc	Short circuit current
Voc	Open circuit voltage
V_{MPP}	Maximum-power voltage
J_{MPP}	Maximum- power current
P_{MPP}	Maximum power
R_s	Series resistance
R_{sh}	Shunt resistance
FF	Fill factor
QE	Quantum Efficiency
EQE	External Quantum Efficiency

IQE	Internal Quantum Efficiency
PCE	Power conversion efficiency
CdTe	Cadmium Telluride
CIGS	Copper-Indium-Gallium-Selenide
QD	Quantum dot
OPV	Organic photovoltaic
DDSS	Dye-sensitized solar cells
PCE	Perovskite solar cell
ETL	electron transport layer
HTL	Hole transport layer
ETM	Electron transport material
ETM	Electron transport material
FTO	Fluorine-doped tin oxide
HOMO	highest occupied molecular orbital
LUMO	lower unoccupied molecular orbital
ZnO	Zinc oxide
CuSCN	Copper(I) thiocyanate
TiO_2	Titanium dioxide
Pb	lead
I	Iodide
Cl	Chlorine
Br	Brom
Sn	Tin
Si	Silicone
Ge	Germanium
In	Indium
Ga	Gallium
Al	Aluminium

B	Bohr
H_2O	Water molecule
Sr	Strontium
Ba	Barium
Rb	Rubidium
Ni	Nickel
Cu	Copper
$MAPbI_3$	Methylamonium lead iodide
FA	Formamidinium
MA	Methylamonium
GBL	Gamma-butyrolactone
DMF	N,N-dimethylformamide
DMSO	Dimethylsulfoxide
CB	Conduction band
CBO	Conduction band offset

Introduction

Energy is one of essential elements for modernization and urbanization. Due to industrialization and increasing wealth in emerging markets, there is a rapidly growing demand for energy. The standard choice to satisfy these demands is fossil fuels, the increase in energy demands entails the depletion of world fossil fuel resources. Moreover, the consumption of fossil energy has a detrimental side effect which is producing greenhouse gases, which has already resulted in an increase of the atmospheric CO_2 concentration and the global warming. Exploring renewable and environmentally friendly alternatives to fossil fuels is one of the most important objectives in energy production. One of the most promising renewable energy sources is solar power, especially solar photovoltaic. Photovoltaic (PV) is a technology that uses semiconducting materials that exhibit photovoltaic effects and convert sunlight into usable electricity, and it is particularly the most promising as the solar power is pollution-free during daily consumption.

Solar cells have received great attention lately. In order to reduced its manufacturing cost and convert sunlight in a more efficient manner than the current-state-of-the art. In this context, a new promising type of solar cells has emerged, which is the Perovskite solar cells. It was named after the main material it is made of. Perovskite are materials described by the formula ABX_3. It has been deemed to have advantageous electrical, structural, optical, and ferroelectric properties which makes it to be an excellent photovoltaic material. The organometal trihalide perovskite as light absorber in solar cells has amazed everyone by obtaining in a short time span significant improvement in power conversion efficiency (PCE). Since the first trying on a sensitized solar cell based on perovskite nanocrystalline particles self-organized in 2009, the PCE of perovskite-based solar cells has rapidly improved from 3.8% to 25.2% over the past 10 years. Compare to conventional silicon solar cell, perovskite-based solar cell has higher energy return on investment due to low material utilization and ability to solution process. Several architectures have been developed for this type of solar cells. Planar junction architecture enabled researchers to achieve a high PCE. Generally, a usual planar perovskite solar cell includes three main layers, where a perovskite film is embedded between an n-type electron-transport layer (ETL) and a p-type hole-transport layer (HTL). The understanding of device operation mechanism is essential for the optimization of the device structure, which leads to the efficiency improvement.

In order to understand the mechanism of the device, it is necessary to study each layer separately and know its effect on the performance of the device. The perovskite solar cell with a n-i-p structure the electron transport layer is the front side of the solar cell, and it may have an impact

on its performance. The work here presented has its focus on the effect of the electron transport layer on the photovoltaic (PV) parameters of the solar cell using the solar cell capacitance simulator (SCAPS) in one dimension.

The first chapter gives an overview of solar cells, their various generations, the most important parameters of a solar cells then focuses on perovskite solar cells in particular.

Chapter 2 offers an outlook over organic inorganic halide perovskite the structure, along with impact over the optical and electrical properties, different fabrication techniques are considered. The materials used as a hole and electrons transport layers. And the different issues in perovskite solar cells.

Chapter 3 summarizes the simulation software and the main parameters used. And discusses the results obtained in this work, drawing the conclusions.

Chapter 1

Technology of solar cells

1.1 Introduction

Solar energy, as a part of renewable energy sources, plays an increasingly important role to meet the world's energy demand, especially in dealing with the climate change issue. Today, photovoltaic (PV) is one of the fastest-growing renewable energy technologies, and is ready to play a major role in the future global electricity generation mix. Based on renewable energy data in 2018 According to international renewable energy agency (ARENA), solar cell or solar photovoltaic (PV) installed capacity is recorded at 480984 MW, came third after hydro and wind power with 8.3% of total Technologies (electricity generation 549833GWh).

1.2 Solar cells

Solar cells are devices which convert solar energy directly into electricity by the photovoltaic effect [1]. The Conversion of solar light into electric power requires the generation of both negative and positive charges as well as a compelling force to drive these charges through an external electric circuit for charge collection. The external circuit can be later connected to any electrical equipment to utilize the generated electrical power. In fact, the photon striking the electron in the solar cell must possess enough energy to excite a valance electron to jump to the conduction band. The energy gap between the conduction band and valance band with the energy supplied to the valance electron by the photon defines the probability of an electron to be in the conduction path and be beneficial for the power generation. The maximum current is determined by the number of electrons being excited to jump to the conduction band per second (see Figure 1.1) [2].

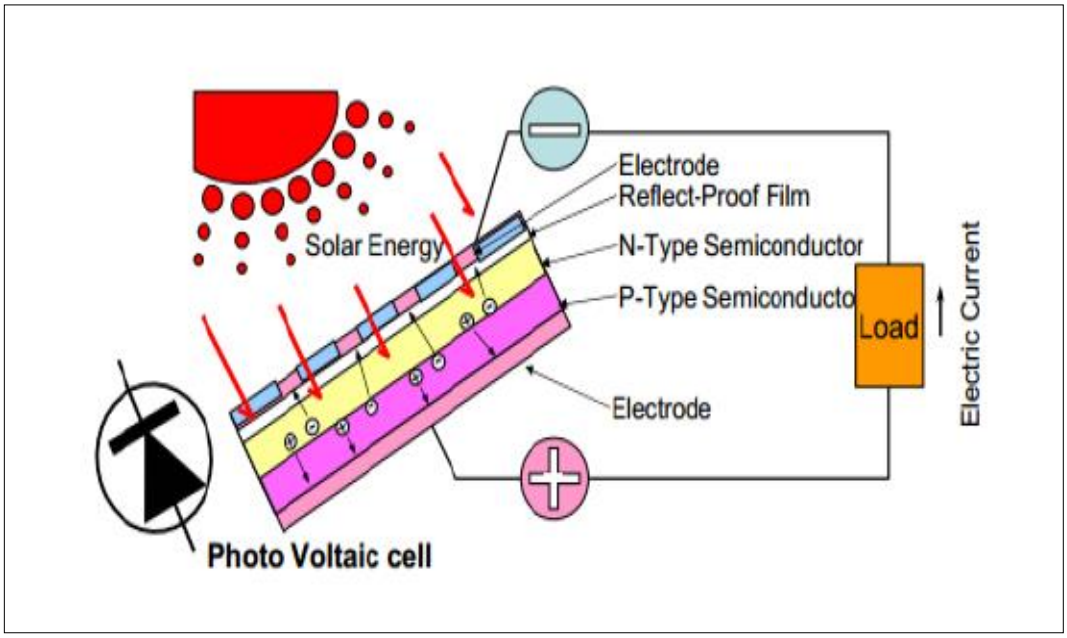

Figure 1.1: Basic Working Mechanisms of solar cell device [3].

In organic semiconductors, with the photon absorption, an exciton is created which is a bound pair of electron and hole. The excitons are neutral in charge and dissociate and diffuse at certain areas called hetero-junctions. The electron carrying the negative charge travels towards the anode and the hole with the positive charge is attracted towards the cathode. After reaching the respective electrodes they are injected into the external circuit and hence fulfilling their purpose to form electrical power and get utilized [2].

1.3 Solar Cell Characteristics

The J-V characteristic of an illuminated solar cell that behaves as the ideal diode is given by equation (1.1).

$$I = I_0 \left[exp\left(\frac{qV}{nkT}\right) - 1 \right] - I_L \qquad (1.1)$$

This behaviour can be described by a simple equivalent circuit in which a diode and a current source are connected in parallel. The diode is formed by a p-n junction. The first term in equation (1.1). Describes the dark diode current density while the second term describes the photo-generated current density [4, 5].

The main parameters that are used to characterise the performance of solar cells are the short-circuit current I_{sc}, the open circuit voltage V_{oc}, the fill factor FF, and power conversion efficiency.

These parameters are determined from the illuminated J-V characteristic. Quantum efficiency also be added.

1.3.1 short circuit current

The short-circuit current (I_{sc}) is the current through the solar cell when the voltage across the device is zero. The flow of $Isc$is due to the generation and collection of light generated carriers. It mainly depends on the number of incident photons as well as the spectrum, area of solar cell, optical properties and the collection probability of photo generated carriers [4]. The graphical representation of Isc is given in Figure 1.2.

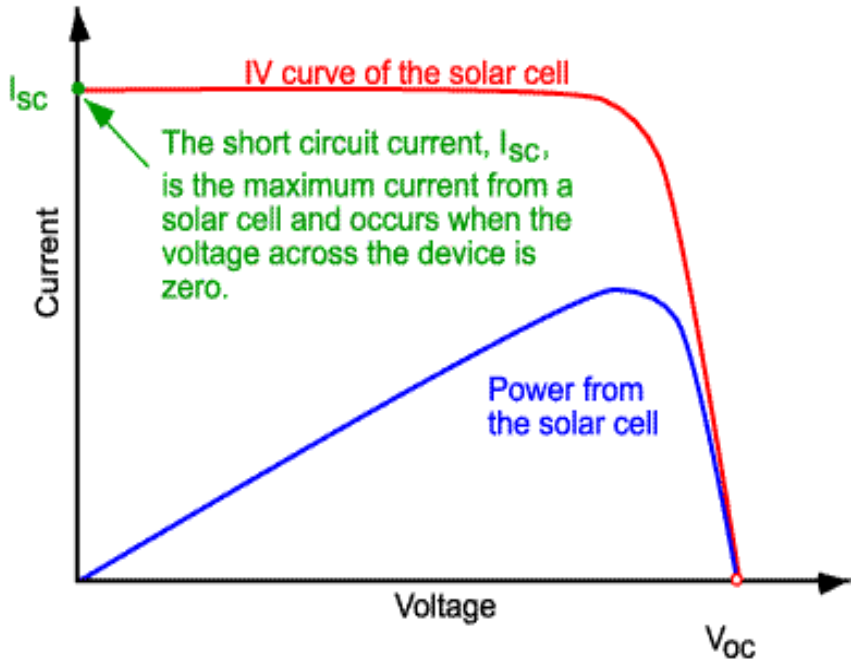

Figure 1.2: I-V curve of a solar cell showing short-circuit current [3].

1.3.2 Open circuit voltage

When a solar cell is an open circuited, and no load is connected across the solar cell then current will be at its minimum (zero) value whereas the voltage will be at maximum value. From solar cell equation, V_{oc}can be derived by setting net current to zero and is given in equation (1.2).

$$V_{oc} = \frac{nkT}{q} ln\left(\frac{I_L}{I_o} + 1\right) \qquad (1.2)$$

From the above equation, it is clear that open circuit voltage depends on I_0 (saturation current) and I_L (light generated current). I_0 depends on recombination in the solar cell. So, V_{oc} can be a measure of the amount of recombination in a solar cell [4]. The graphical representation of Voc is given in Figure 1.3

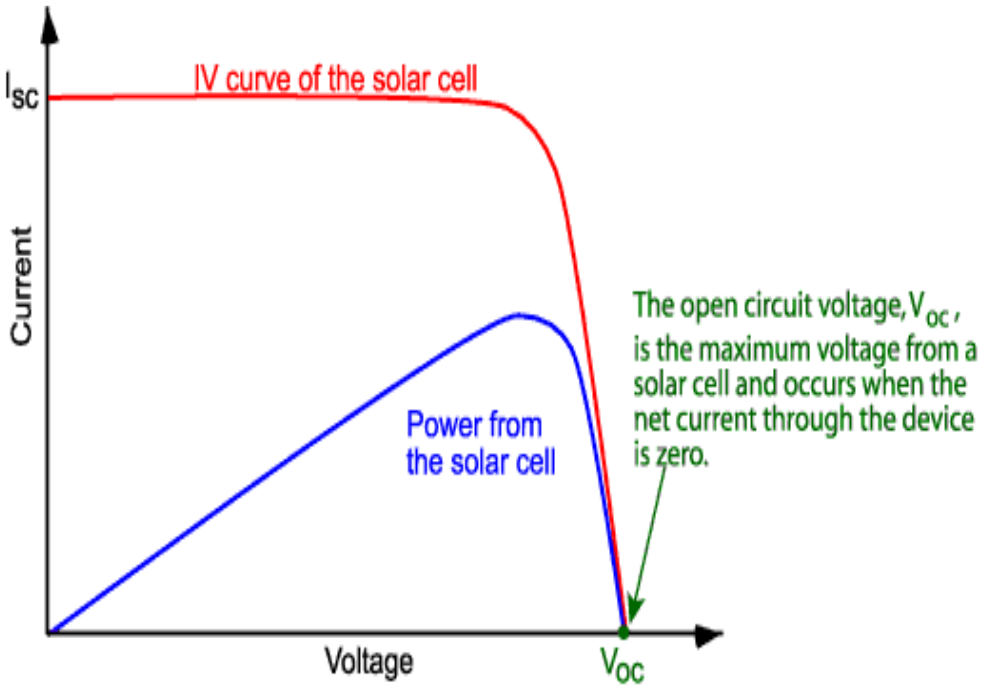

Figure 1.3: I-V curve of a solar cell showing the open-circuit voltage [3].

1.3.3 Fill factor

One of the measurements that determines the quality of a solar cell is fill factor (FF), which is derived by equating the maximum power (P_{MPP}) to the theoretical power (P_t). Where power (P_t) would be output at both the open circuit voltage (V_{oc}) and short-circuit current (I_{sc}) as given in equation (1.3) [4]. Fill factor can be interpreted graphically as the ratio of the rectangular areas depicted in Figure 1.4.

$$FF = \frac{V_{MPP} \cdot J_{MPP}}{V_{oc} \cdot J_{sc}} = \frac{P_{MPP}}{V_{oc} \cdot J_{sc}} < 1 \qquad (1.3)$$

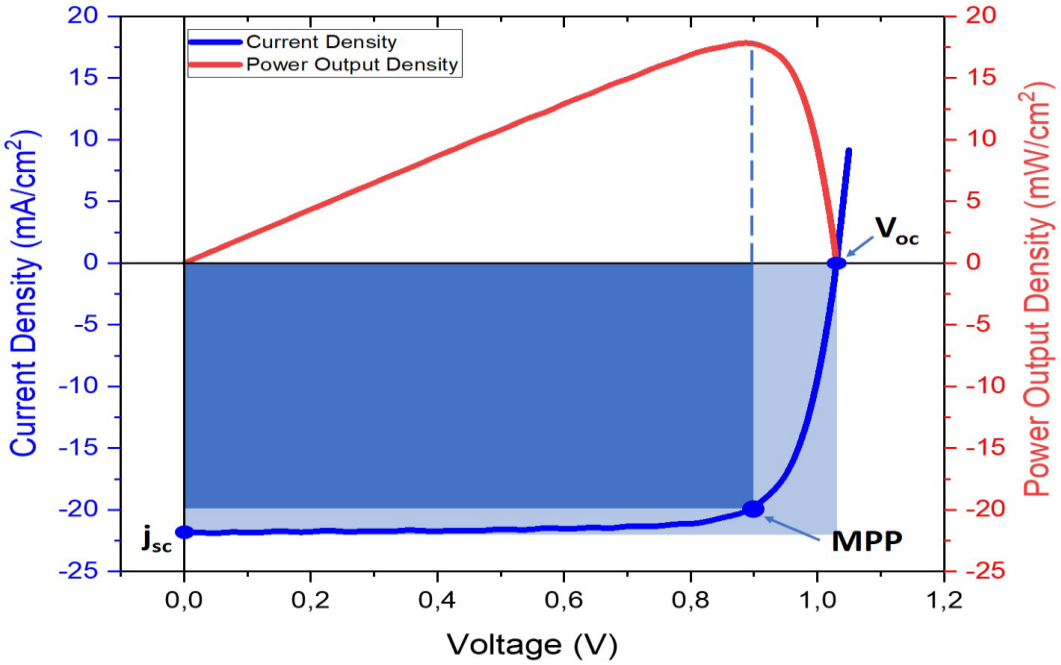

Figure 1.4: Typical current density-voltage curve (JV curve) and corresponding electrical power output density from a solar cell. Denoted are the short-circuit current density (J_{sc}), the open circuit voltage (V_{oc}), and the maximum power point at (V_{MPP}), which generates the maximum power output (P_{MPP}). Adapted from [6].

1.3.4 Quantum efficiency

The ‘‘quantum efficiency’’ (QE) is the ratio of number of carriers collected by the solar cell to the number of photons of a given energy incident on the solar cell. The quantum certain wavelength is absorbed and the resulting minority carriers are collected, then the quantum efficiency at that particular wavelength is unity. A quantum efficiency curve for an ideal solar cell is shown in Figure 1.5. While quantum efficiency ideally has the square shape, the quantum efficiency for most solar cells is reduced due to recombination effects. The same mechanisms which affect the collection probability also affect the quantum efficiency [3, 7, 8].

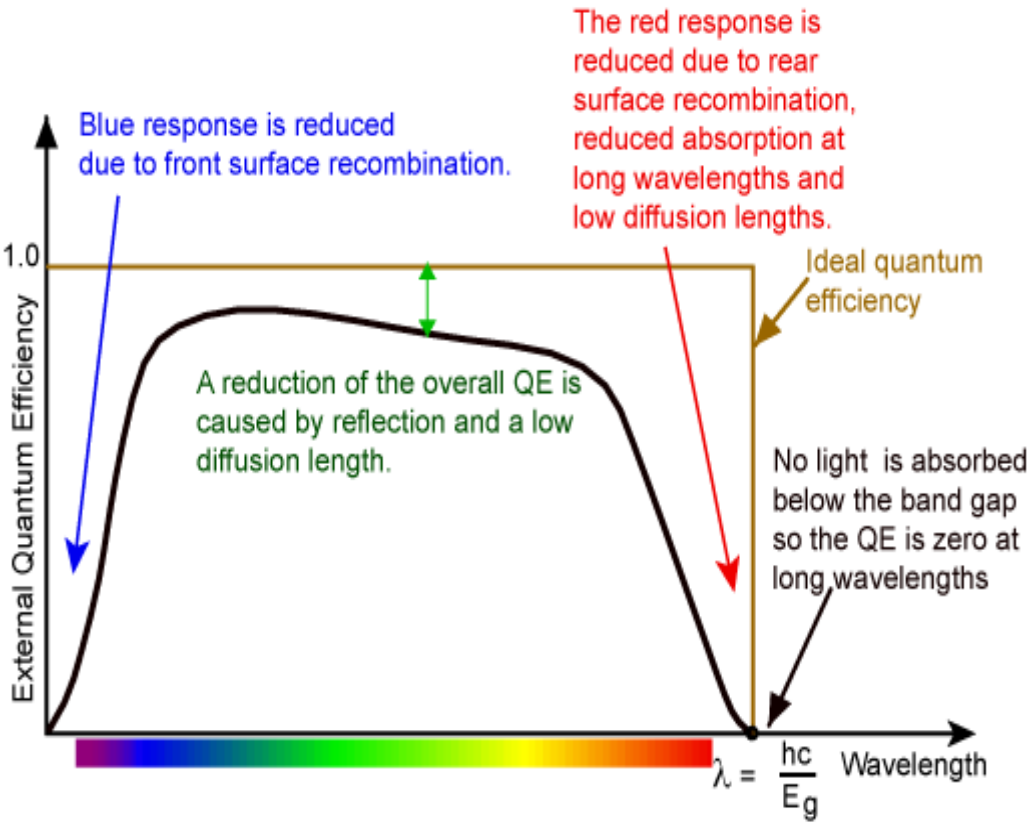

Figure 1.5: The quantum efficiency of a silicon solar cell. Quantum efficiency is usually not measured much below 350 nm as the power from the AM1.5 contained in such low wavelengths is low [8].

There are two types of QE: external quantum efficiency (EQE) and internal quantum efficiency (IQE). EQE is the ratio between the number of charge carrier collected by solar cells with the number of incident photons while IQE only takes into account the absorbed photons. This explains why the value of IQE is always higher than EQE [7, 9]. Both of EQE and IQE are given by equations (1.4) and (1.5).

$$EQE(\lambda) = \frac{Jsc(\lambda).h\nu}{qP_{in}(\lambda)} = \frac{hc}{q\lambda}SR(\lambda) \tag{1.4}$$

$$IQE(\lambda) = \frac{1}{1-R(\lambda)}EQE \tag{1.5}$$

Where SR is the spectral response, and it is a ratio between the current generated by the cell and the incident power. h is Planck's constant, c is the light speed, q is the electronic charge, and λ is the wavelength [7].

1.3.5 Power conversion efficiency

Power conversion efficiency is the most frequently used parameter to relate the performance of two solar cells and is termed as PCE. It is defined as the ratio of output power from a solar cell to the input power from the sun. The PCE depends on parameters like incident sunlight intensity, solar cell working temperature and spectrum type [4]. Mathematically expressed in equations.

$$PCE = \frac{P_{max}}{P_{in}} \tag{1.6}$$

$$P_{max} = V_{oc} I_{sc} FF \tag{1.7}$$

$$PCE = \frac{V_{oc} I_{sc} FF}{P_{in}} \tag{1.8}$$

1.4 Generation of solar cells

Many new kinds of solar cells have been developed in the recent decades. Solar cells are categorized into three generations [10]. The worldwide research-based different of PV technologies having the best power conversion efficiencies from 1976 to 2019 are shown in Figure 1.6. This information chart was published by National Renewable Energy Laboratory (NREL) of the United State Department of energy. The power conversion efficiency of different types of solar cells has been improved with the passage of time. The classification is based on the nature of the material, the maximum efficiency reachable, and the cost of each type (Figure 1.7) [5].

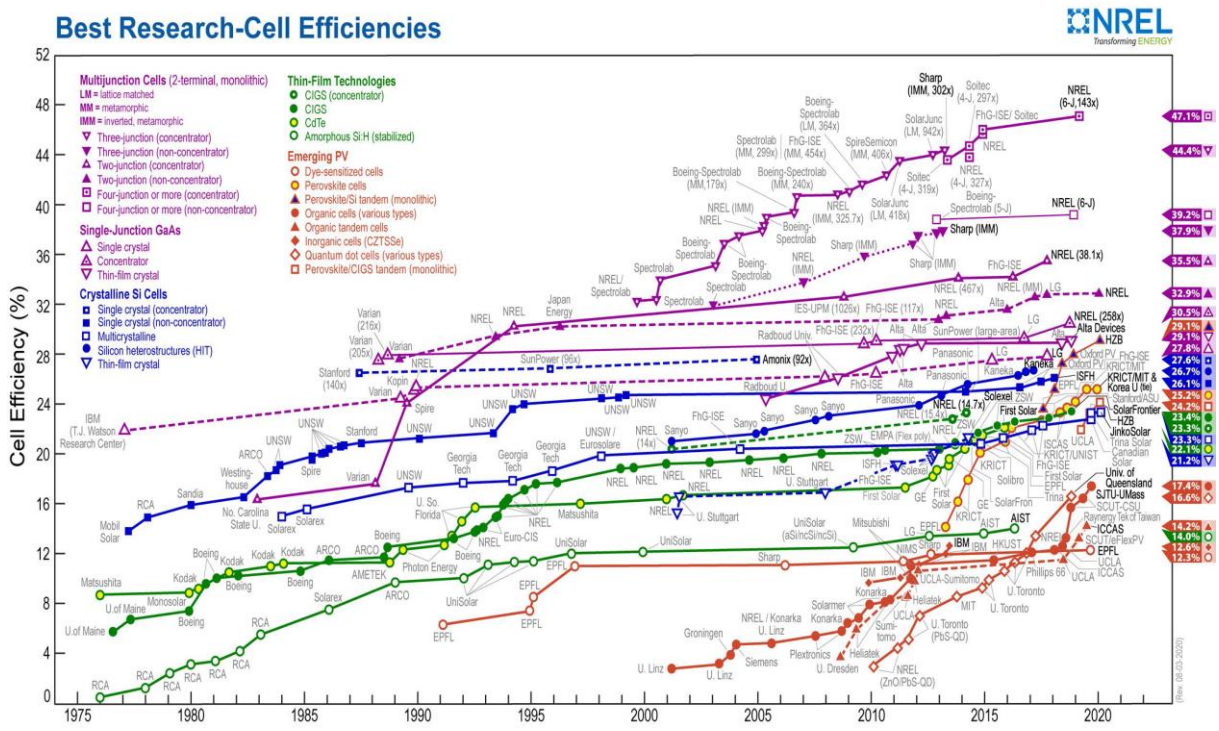

Figure 1.6: Best research-cell efficiencies for the multitude of different solar cell technologies [11].

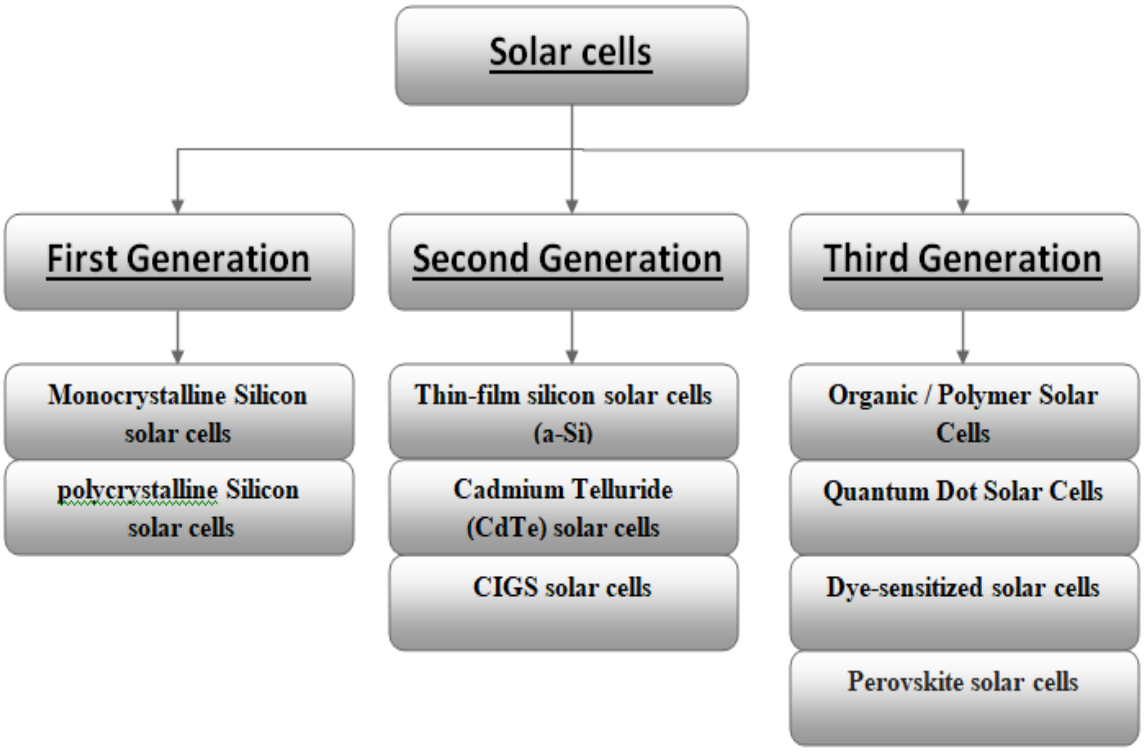

Figure 1.7: Classification of various solar cell technology.

1.4.1 First generation

The first generation solar cells are silicon solar cells, including polycrystalline silicon solar cells and monocrystalline silicon solar cells. They have usually a Large area, high quality and single junction devices, their theoretical limit on efficiency for single junction is 33% [5, 12].

1.4.1.1 Monocrystalline Silicon

The monocrystalline silicon solar cell is made of a large single crystal of pure silicon. This single crystal is mostly fabricated owing to the Czochralski method [13]. The efficiency of mono-crystalline silicon solar cells lies between 25% - 26% [14], but this type of solar cells is very expensive, because they are cut from cylindrical ingots, do not completely cover a square solar-cell module without a substantial waste of refined silicon [5].

1.4.1.2 Multicrystalline Silicon

Polycrystalline silicon solar cells are currently the most popular solar cells because the processing of polycrystalline Si solar cells is more economical, where the arrangement of the cell modules is typically rectangular, but Polycrystalline silicon is much less pure than the single crystalline silicon. The efficiency of this type of silicon solar cells lies between 20% - 22% [5, 9, 13].

1.4.2 Second Generation

Second-generation solar cells are also known as thin-film solar cells because they are made from layers only a few micrometers thick. This generation is considerably cheaper to produce than first generation cells and does hold promise of higher efficiencies. There are basically three primary types of thin film solar cells that have been commercially developed [9, 12].

1.4.2.1 Thin-film silicon solar cells

Both in the amorphous and the microcrystalline form, constitutes at present one of the most promising material options for low-cost, large-scale terrestrial applications of photovoltaic because it allows for low-temperature fabrication processes PECVD [15].

Amorphous silicon solar cells are not based on a p-n junction like wafer based c-Si solar cells. Instead, they are based on a p-i-n junction, which means that an intrinsic layer is sandwiched between thin p-doped and n-doped layers for create an electric field that helps moving the carriers. The performance of solar cell can be improved when using tandem and even triple layer devices that contain p-i-n cells. The best stabilized module efficiency is ~ 10% [4, 9].

1.4.2.2 Cadmium Telluride (CdTe)

The CdTe thin film cells have gone through a rapid development in recent years. due to their competitiveness in terms of cost (the first PV technology at a low cost), high conversion efficiency, and the available manufacturing processes. The CdTe solar cells are generally constructed by sandwiching between cadmium sulphide layers to form a p-n junction diode [13, 16].

The CdTe is most attractive material for designing of thin-film solar cells, because it has an excellent direct band gap of ~1.45 eV with high absorption coefficient, that make its efficiency operates in the range 21.4%. but this CdTe technology is limited because the main issues of the toxic Cd based materials [5, 14].

1.4.2.3 CIGS solar cells

CIGS solar cells are receiving worldwide attention for solar power generation. They are considered as the most promising cells, because their conversion efficiency (23.35%) is coming close to the conversion efficiency of poly-Si cells, and they showed a very good stability in outdoor tests (without a considerable degradation) [14, 17, 18].

The compound semiconductor copper-indium-gallium-selenide (CIGS) as the basis material satisfies the requirements of thin film solar cells. It is a direct gap semiconductor with high absorption coefficient [18].

1.4.3 Third Generation

Principally, due to high costs of first generation solar cells and toxicity and limited availability of materials for second generation solar cells, a new generation of solar cells emerged. This generation is inherently different from the previous two generations because they do not rely on the p-n junction design of the others [12].

The goal of course is to improve the solar cells by making solar energy more efficient over a wider band of solar energy, less expensive and without any toxicity, in order to achieve these high efficiencies, many concepts have studied in this last years. This generation of solar cells includes organic thin film (polymer solar cells), dye-sensitized solar cells, perovskite solar cells and quantum dot solar cells [3, 12].

1.4.3.1 Organic / Polymer Solar Cells

Organic solar cells are studied extensively for their potential as solution-processable, light weight, low cost, large area energy generators, and more flexible solar cells. Organic or polymer cells are classified as such because the active layers of the cell are made of completely organic materials such as polymers and small-molecule compounds [5].

Organic solar cells can have many typical architectures such as bilayer structure or a bulk-heterojunction structure. OPV module efficiencies are now in the range 8% to 11% for commercial systems [14, 19].

1.4.3.2 Quantum Dot Solar Cells

Also known as nanocrystal based solar cells, and it is just a name of the crystal size ranging typically within a few nanometers (exciton diffusion length). Quantum dots are a special class of semiconductors composed of periodic groups of II-VI, III-V, or IV-VI materials [13, 20, 21].

Quantum dots (QDs) have the advantage of tunable bandgap as a result of size variation as well as formation of intermediate bands, and it can be moulded into a variety of different types, in two-dimensional (sheets) or three-dimensional arrays. Generally, a photon creates one electron-hole pair. However, when a photon strikes a QD made of the similar semiconductor material, numerous electron-hole pairs can be formed, usually 2 or 3, also 7 has been observed in few cases. The theoretical efficiency limit of this technology is estimated to be 63% [13, 22, 23].

1.4.3.3 Dye-sensitized solar cells

Cells are also known Grätzel cells named after the developer, the DSSC differs from other solar cells types both by its basic construction and the physical processes behind its operation, the typical DSSC configuration combines solid and liquid phases (photoelectrochemical cells) [5, 24].

The DSSC device consists of four components: semiconductor, a dye sensitizer, redox electrolyte and a counter electrode (see Figure 1.8). Dye-sensitized solar cells demonstrate specific advantages over other photovoltaic devices, because of their high efficiency (12%), low cost, simple fabrication procedures, environmental friendliness, transparency, and good plasticity. However, there are certain challenges like degradation of dye molecules under heat and *UV* light and stability issues because of liquid electrolytes. All these problems make the lifetime of DSSC very short (five years) [14, 25].

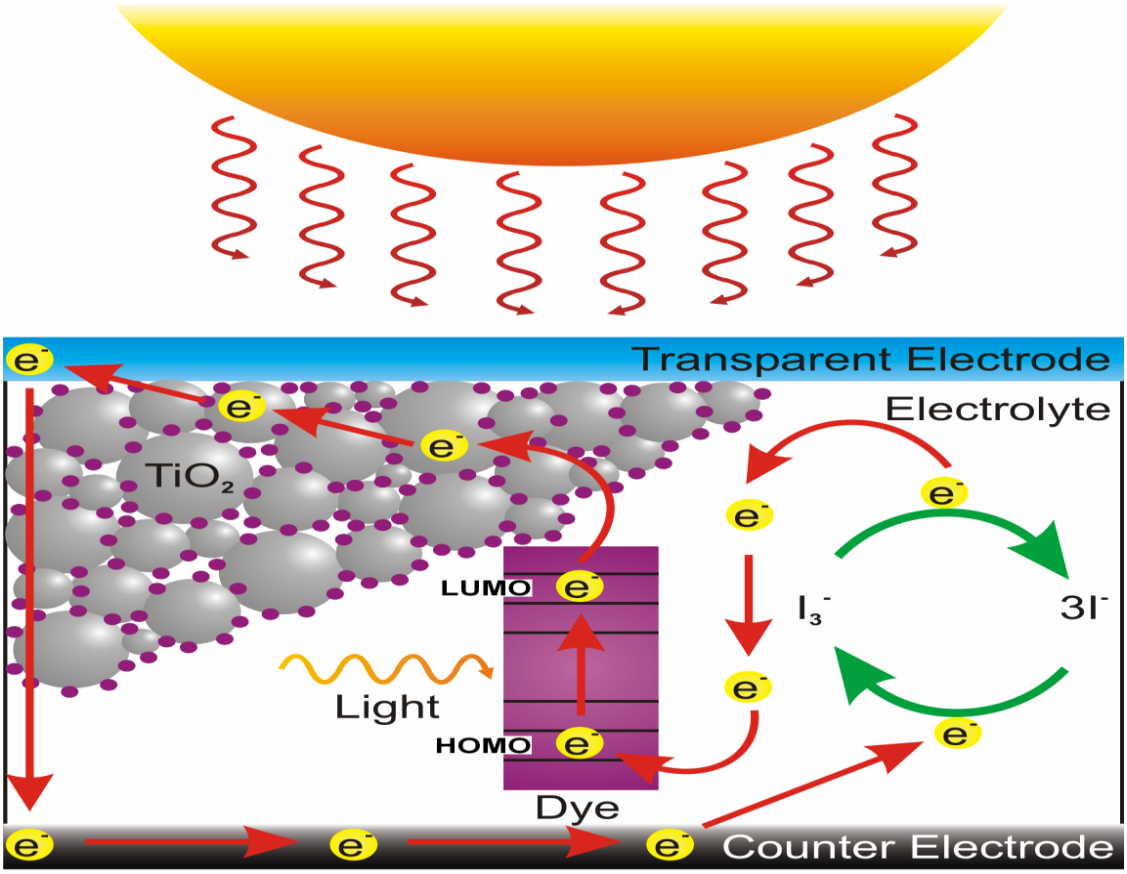

Figure 1.8: Structure and operation of a dye-sensitized solar cell. The incident light excites an electron in a dye molecule into a higher state. Such an excited electron tunnel onto a TiO_2 molecule. The electron then diffuses to the end of the electrode, enters the external circuit and re-enters the cell through the opposite electrode. The oxidized dye molecule is reduced by the electrolyte and the electrolyte is reduced by the re-entering electron [25].

1.4.3.4 Perovskite solar cells

The past decade emerged a new type of solar cells that is called perovskite solar cells. perovskite solar cells are stem from dye-sensitized solar cells. The base technology for this type of solar cells is solid-state sensitized solar cells that are based on dye-sensitized Gratzel solar cells, perovskite

solar cells are a promising photovoltaic technology. Perovskite solar cells (PSCs) have attracted tremendous interest because of their rapid improvement in power conversion efficiency (PCE) from the initial PCE of 3.8% in 2009 for the first prototype to the certified PCE of 25.2% in 2019 [3, 26-28].

The photovoltaics of organic–inorganic lead halide perovskite materials have shown rapid improvements in solar cell performance, surpassing the top efficiency of semiconductor compounds such as CdTe and CIGS (copper indium gallium selenide) used in solar cells in just about a decade, although they lag behind silicon photovoltaics, which hold a 26.6% record - efficiency [28, 29].

Indeed, a number of companies and research centers are devoted to technology transfer from laboratory to market, working on device stability and reliability, up-scaling and compatibility of the cell manufacturing with industrial processes, such as roll-to-roll deposition. Recently, the U.S. Department of Energy (DOE) announced $20 million in funding to advance perovskite solar photovoltaic technologies. To be competitive in the marketplace, perovskite's long-term durability must be tested and verified [30].

1.4.3.4.1 Working Principle of a Perovskite Solar Cell

For Perovskite solar cells utilize perovskite structured light absorbers for photovoltaic activity. The photovoltaic system has three main functioning steps: (1) absorption of photons followed by free charge generation, (2) charge transport, and (3) charge extraction[31]. When sunlight falls on a PSC, the perovskite absorbs light, excitons are generated, and charge carriers (electrons and holes) are produced upon exciton dissociation. Exciton dissociation occurs at the interface between the perovskite layer and the charge-transporting layer. When the electron is separated from the hole and injected into the electron transporting layer (ETL), it migrates to the anode which is in most cases fluorine-doped tin oxide (FTO) glass. Simultaneously, the hole is injected into the hole transporting layer (HTL) and subsequently migrates to the cathode (usually metal). It means high mobility for electrons in the ETM layer, high mobility for holes in the HTM layer, and appropriate band offsets between ETM layer/perovskite layer/HTM layer that are necessary for high efficiency. The electrons and holes are collected by working and counter electrodes respectively and transported to the external circuit to produce current [3, 31-33].

The energy levels should be properly studied for each layer. Because the excited electrons and holes seeking to recombine in order to minimize the total energy. But the charge carriers are also

energy conservers, which mean they will always take the path of minimum resistance. This is done by having the level ETLs LUMO (lower unoccupied molecular orbital) a bit lower than the active layers LUMO which creates a more attractive way for the electron to go. The same is for the level HTLs HOMO (highest occupied molecular orbital) that needs to be a bit higher than the active layers HOMO which creates a more attractive way for holes to go. This is the same for every layer in the cell, each layer has either higher HOMO or lower LUMO for the charge carriers transportation chain (Figure 1.9) [34].

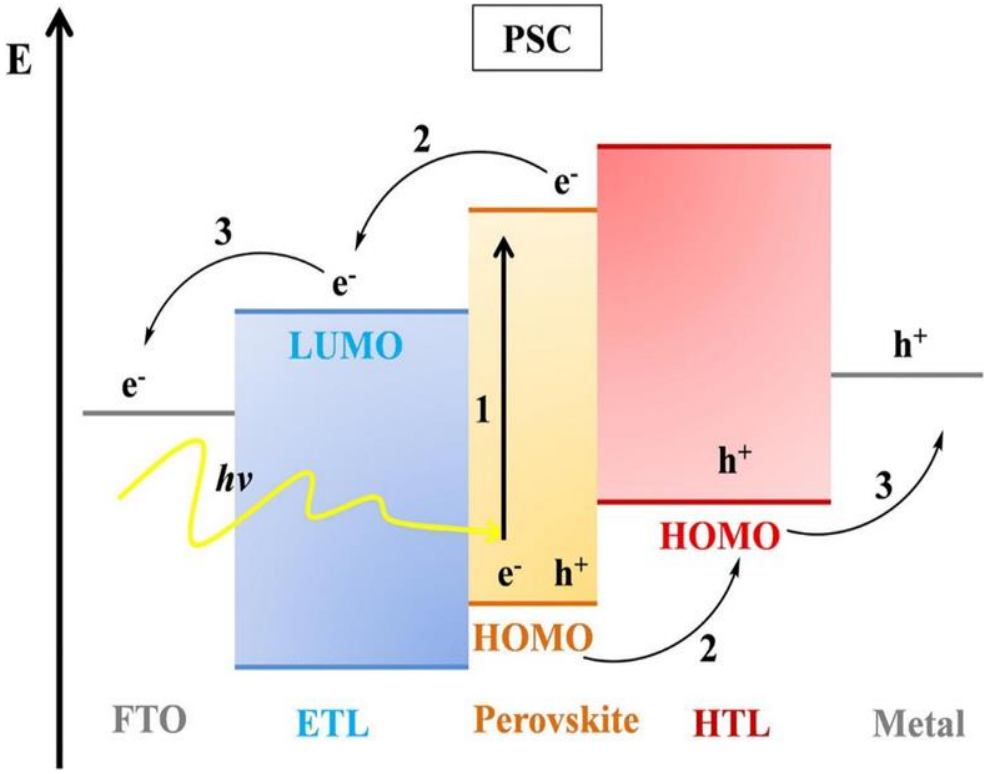

Figure 1.9: Band diagram and operation principle of perovskite solar cell [31].

1.4.3.4.2 Device Structure for Perovskite Solar Cell

The interest increased in perovskite solar cells and developed more, when the liquid electrolyte was replaced with a solid-state material which is called mesoscopic device structures [26, 35]. Where the planar architecture is an evolution of the mesoscopic structure, where the perovskite light-harvesting layer is sandwiched between the electron (ETM) and hole transporting materials (HTM) (see Figure 1.10.A). The absence of a mesoporous metal oxide layer leads to an overall simpler structure. It is possible to achieve a high efficiency without the mesoporous layer by carefully controlling the interfaces between the different layers that make up the PSC (the

perovskite light absorber layer, the electron transporting layer, the hole transporting layer, the electrodes) [36-38]. The planar device structure developed in which the perovskite absorber is sandwiched between the electron (ETM) and hole transporting materials (HTM), the n-i-p is called as normal device structure (see Figure 1.10.B) and p-i-n structure is also called as inverted device structure (see Figure 1.10.C). Simply, depending on the position of the ETM and HTM [39, 40].

Moreover, the optimization of each layer with maintaining their charge mobility, electron balance and optical transmittance becomes typically necessary steps in the fabrication of efficient n-i-p (regular planar) and p-i-n (inverted planar) hybrid structures of PSCs [41].

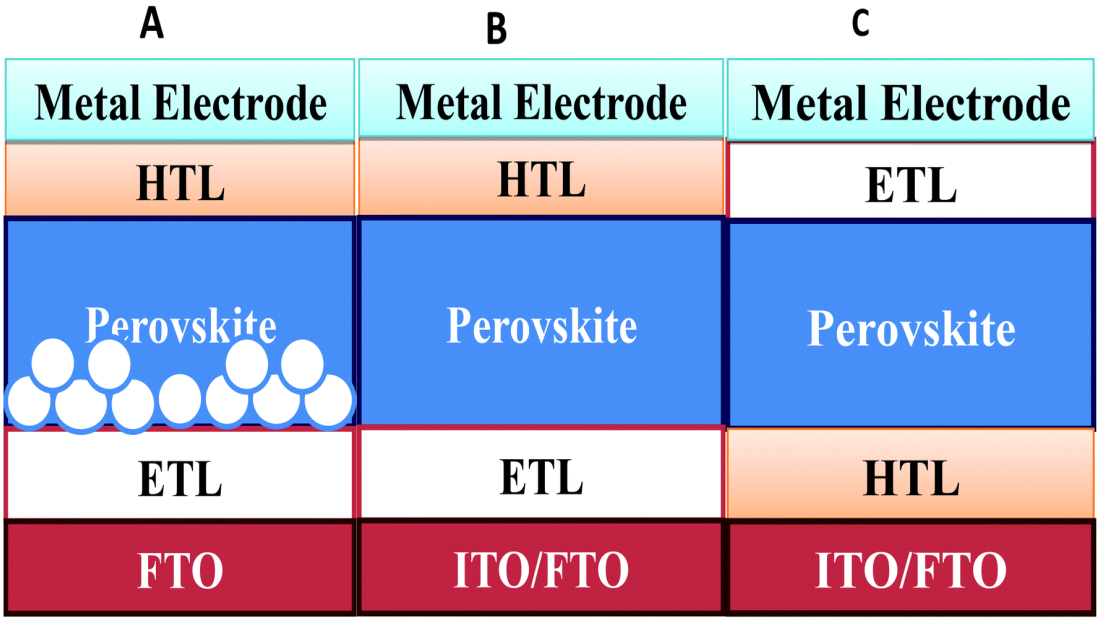

Figure 1.10: Generic structures conventional mesoporous(A), and n-i-p (B)/ inverted p-i-n (C) planar perovskite solar cells [42].

1.4.3.4.3 Transport layers Properties

The ETL, HTL and the perovskite layers are the path that photo-generated carriers must travel before being collected. A good understanding of the effects of each of the layers in the performance of the devices is critical for optimization [43].

Hole Transport Layer

The use of a hole transport material (HTM) remains indispensable in perovskite solar cells [44]. the HTM Serves various purposes in PSCs: (i) it is a physical energetic barrier between anode and perovskite layer that blocks the electron transfer to anode [45], (ii) it improves the hole transfer

efficiency [46, 47], (iii) . The presence of an HTM layer has shown to improve surface coverage compared to that of a perovskite layer only [48]. For the efficient hole extraction at the perovskite-HTM interface, is should be (i) high hole mobility to reduce losses during hole transport to the hole-collecting contact, (ii) compatible ionization potential with that of the perovskite (i.e. highest occupied molecular orbital (HOMO) or valance band maximum (VB) almost matching that of the perovskite absorber so as to minimize injection losses), (iii) high thermal stability and resistance to external degradation factors such as moisture and oxygen for a long term durable PV operation [47]. There is a wide range of HTMs employed such as organic (small molecules and polymers) and inorganic HTMs [45].

Electron Transport Layer

For any material to be employed as electron transport layer in perovskite solar cells, the material must satisfy few important properties. Those properties are: (i) Conduction band of the ETL material should be less than the LUMO level of the perovskite material (ii) high electron mobility (iii) higher band gap [49]. Organic-Inorganic materials are used in perovskite solar cells as electron transport materials widely. With high electron mobility, they can effectively carry out the transmission of electrons. The nature of the material determines their strengths and weaknesses [50]. N-type semiconductor is usually used in electron transport materials, which can make the free electron concentration greater than hole concentration [49, 50].

Chapter 2

Perovskite solar cell

2.1 Introduction

The emergence of perovskite solar cell marks a revolution in the field of photovoltaics, promising the elusive combination of low cost and high efficiency. The perovskite solar cell are kind of solar cell which use perovskite based material as the light absorbing layer. In general, PSC consists of three parts of layers which include ETM, perovskite, and HTM. The charge-transporting layer plays an important role in enhancing selective charge collection in the perovskite solar cells [51, 52].

2.2 CuSCN as hole transport material

Background on CuSCN

CuSCN a molecular metal pseudo-halide (polyatomic groups that incorporate a pseudo-halogen anion such as thiocyanate) of singly ionized copper behaves like halide ions in chemical reactions [53, 54], it is an intrinsic semiconductor, which exhibit p-type conductivity. A material copper (I) thiocyanate can exist in two forms: α-phase and β-phase. The α- phase has an orthorhombic crystal lattice and β- phase more stable readily available can be as a hexagonal or rhombohedral structure (Figure 2.1) [53-56]. Structure β-CuSCN has layers of SCN ions separating the plains of Cu atoms and a strong Cu-S bond that interconnects three dimensionally and this structure is more stable [57].

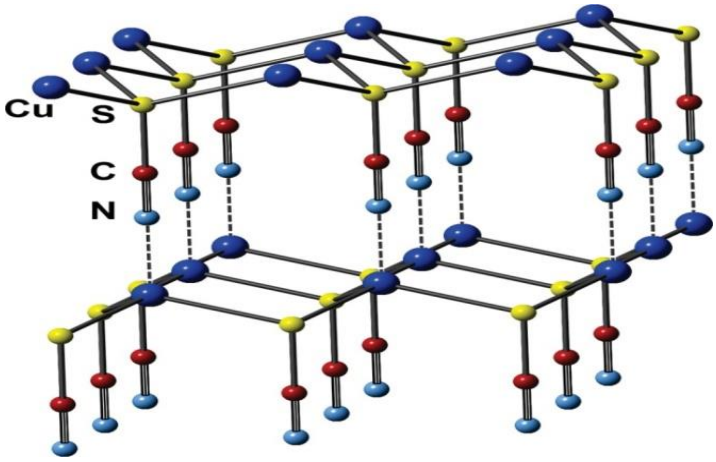

Figure 2.1: Structure of β-CuSCN [54].

Properties of CuSCN

Copper(I) thiocyanate (CuSCN) demonstrated good potential as a hole transport material, in field optoelectronics research. The material CuSCN is readily available, inexpensive and can be processed at low temperatures [53]. It is well known that CuSCN is an inorganic intrinsic semiconductor which exhibit p-type conductivity. In addition to that it is distinguished high optical transparency over the visible to the near infrared region show in (Figure 2.2). Which facilitates photoactive materials to absorb more light for generating higher photo current in solar cells. In addition to its large bandgap (>3.4 eV), high hole mobility (0.01-0.1 $cm^2V^{-1}s^{-1}$), and high chemical stability [58, 59], finally it possesses a deep valence band energy level, that can help to maximize open circuit voltage (V_{OC}) [55, 60].

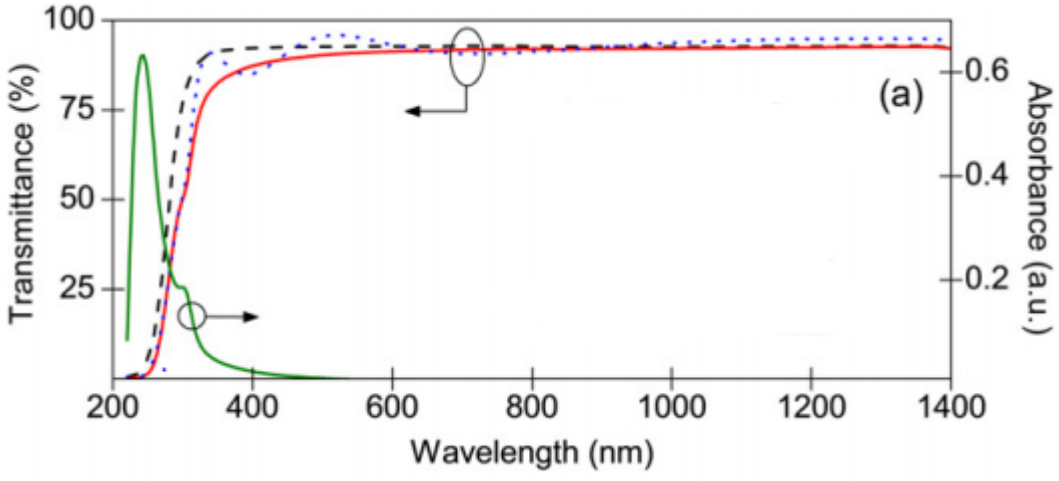

Figure 2.2: Transmittance and absorbance spectra from a thin-film of CuSCN on a glass [53].

2.3 Perovskite (Active layer)

2.3.1 Structural properties of hybrid organic-inorganic perovskite

The perovskite returns to the crystal structure of calcium titanate oxide mineral ($CaTiO_3$), which was discovered by the German mineralogist Gustav Rose in 1839. From a rock sample of the Ural Mountains of Russia and who determined its physical properties and chemical composition. He gave the name perovskite as a tribute to the Russian count Alexeïevitch Perovski, who was also a mineralogist [51].

The general chemical formula of the perovskite structure is ABX_3, A and B are two cations of very different sizes whereas "X" is anion, often be oxygen or halogen. A is a elements monovalent cation which can be inorganic such as (Rb^+, Cu^+) or can be organic (CH_3NH_3 methylammonium, $CH_3(NH_2)_2^+$ formamidinium). B is a bivalent cation (Cu^{2+}, Ni^2, Ge^{2+}, Sn^{2+}, Pb^{2+}, Sr^{2+}, Ba^{2+}). In the ideal perovskite structure A^+ cations are at the corners of a cube, the anions X are in the middle of each faces, and B^{2+}cations are in the middle of the octahedral sites formed by the anions (Figure 2.3) [52, 61-64].

Organic-inorganic halide perovskite have attracted a great deal of attention to the field of solar cell, due to their unique structures and wide applications in electrical, mechanical, optical, magnetic and electronic devices. Organic-inorganic hybrid material has shown the possibility to combine the properties of organic component and the inorganic component, resulting in having marvellous characteristics with high efficiency, light weight, and low-temperature processability. In addition to that hybrid perovskites possess extremely high absorption coefficients [65-67]. For example, $CH_3NH_3BX_3$ (CH_3 NH^{+3}, also called MA^+) (B=Pb, Sn and X=Cl, Br or I), it was used in 2009 as the first working hybrid perovskite solar cell. By methylamonium lead iodide ($CH_3NH_3PbI_3$)showing a surprising efficiency of about 3.8% [68], it is now considered a proven fact that methylamonium lead iodide behaves mostly as an intrinsic semiconductor, $MAPbI_3$ is able to transport both electrons and hole [69].

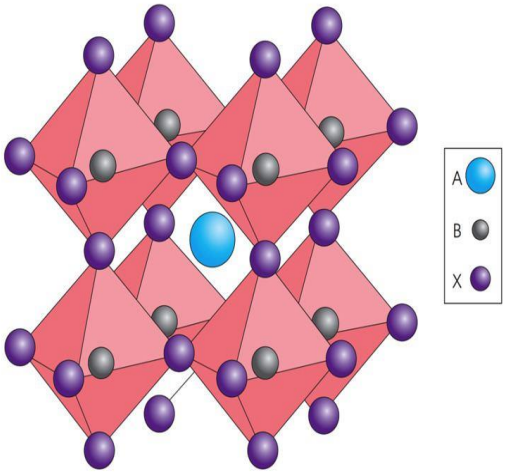

Figure 2.3: the general formula of the perovskite structure ABX_3 on right [65].

The perovskite formation tendency can be depicted by using gold Schmidt tolerance factor (t) which is an indicator for the stability of Structure ABX_3 and the degree of distortion of crystal structure [64]. It is the ratio of the distance between A and X to the distance between B and X, which is given by in equation (2.1).

$$t = \frac{R_A + R_B}{\sqrt{2}(R_B + R_X)} \tag{2.1}$$

Where R_A, R_B and R_X represent ionic radii of A, B cation and X anion respectively. The perovskite structure varies according to the tolerance factor, where the ideal cubic perovskite α phase structure, would have a $0.89 < t < 1$ therefore in order to satisfy the ideal tolerance factor ($t \approx 1$), the A-site ion must be much larger than the B-site ion ($R_A > R_B$). Lower values of t ($t < 0.89$), lead to less symmetric tetragonal (β phase) or orthorhombic (γ phase) structures. On the other hand, high values of t ($t > 1$) could destabilize the 3D B–X network, leading to a two-dimensional (2D) layer structure [3, 31, 65].

However, it is not enough to deduce the probable crystallographic structure of perovskite materials by only considering tolerance factors. Therefore, the octahedral factor "μ" is used as an additional indicator to predict the formation of perovskite structure, should lie between $0.44 < \mu < 0.90$ for stable perovskite structures and is given by equation(2.2) [65, 70, 71].

$$\mu = \frac{R_A}{R_X} \tag{2.2}$$

Whereas the tolerance factor (t) and the octahedral factor (μ) are two important factors to quantify the structure and stability of perovskite [26].

2.3.2 Opto-electronic properties

The great interest in this class of perovskite lies in the remarkable opto-electronic properties of this material which can also be solution-processed. Numerous research efforts on both PSC efficiency improvements and deeper understanding about perovskite materials, outstanding electrical and optical properties, such as largely-tuneable band gaps for light absorption, high absorption coefficients, large carrier diffusion lengths, great carrier mobility, have been-established during the past few years [72, 73].

Bandgap is a very important parameter for a photovoltaic material, this is because, according to Shockley–Queisser limit, the maximum theoretical efficiency that can be achieved is dependents on bandgap of the material. $CH_3NH_3PbI_3$ is an intrinsic semiconductor with a band gap of 1.55 eV [73, 74]. Thus, the absorption onset is close to 800 nm (with absorption coefficient ~10^5 – $10^6 cm^{-1}$), with strong absorption of the visible spectrum. As a result, thin absorbing films (~300-600 nm) are usually considered adequate to absorb the light in a solar cell and for good charge collection [74-76] . Additionally, the photo-induced excitons rapidly dissociate into free charge carriers at room temperature due to their weak binding energy (~50 meV). These free carriers have a small effective mass, therefore resulting in carrier mobilities of 24±7 cm^2/Vs for electrons and 105±35 $cm^2/V.s$ for holes. The recombination of these carriers occurs on a timescale of hundreds of nanoseconds, and thus resulting in long carrier-diffusion lengths ranging between 100 nm and 1 μm [77, 78]. Another attractive property of perovskites is the possibility to tune their bandgap by varying the combination of the cationic and anionic components of the crystal structure. This is done to enable the realization of colorful solar cells for various building applications as well as increasing the coverage range of the visible solar spectrum [79].

2.3.3 Deposition methods

Techniques and various methods have been established to fabricate an improved quality of perovskite film. Which relied on the same principle, the combination of an organic and inorganic component. In the one-step deposition or spin coating method, is the most common in deposition methods due to its easier operation and low cost. The perovskite is prepared in a

common solution typically precursor solution was prepared with organic halide (MAI/FAI, methylammonium/formamidinium iodide) and inorganic halide Pb_2 [80-82], dissolved in gamma-butyrolactone (GBL), N,N-dimethylformamide (DMF), dimethyl sulfoxide (DMSO) [83, 84], or a combination of two or all three solvents, are then spin coated (Figure 2.4.a).

The two-step deposition method was developed for deposition of perovskite films in a low temperature, as a second way to improve deposition in one step that results in poor surface coverage showing non-uniformity. The two-step deposition method does not required a complete precursor preparation but separates the coating of PbI_2 and MAI, a thin film is first deposited using metal halide PbI_2 precursor using spin coating process mostly and then the film coated substrate is dipped into the second precursor solution MAI the final perovskite films would be formed after proper baking. Although steps become more complicated [3, 64, 80, 82, 85] (Figure 2.4.b).

It has also been other kinds of modified deposition methods were developed used to deposit perovskite films, among them vapor-assisted solution method that can be considered as a modified two-step method assisted process to deposit perovskite film. The incorporation of MAI was done via vapor deposition technique over the PbI_2 seed layer which is deposited by spin coating, where the MAI vapor was formed at 150 ^{0}C, without any problems of incomplete conversion and limited Solubility (Figure 2.4.d). Perovskite films with full surface coverage, small surface roughness, and grain size up to microns were obtained [64, 81, 86]. As such vapour deposition method (dual-source) which deposition of organic and the inorganic precursor at the same time produces superior uniformity for perovskite films, which subsequently results in substantially improved solar cell performance [82, 87] (Figure 2.4.c).

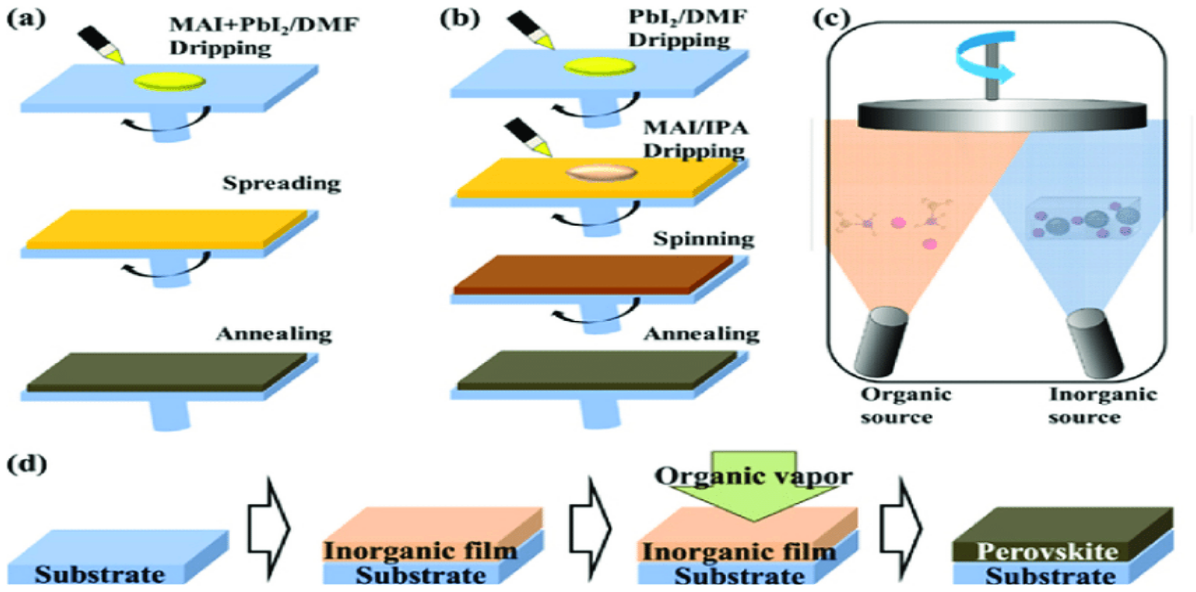

Figure 2.4: Fabrication methods of a perovskite films:(a) one-step spin-coating method; (b) two step deposition method; (c) dual-source vapor deposition; and (d) vapor-assisted solution process [88].

2.4 Zinc oxide as electron transport material

Back ground for ZnO

Recent studies have revealed that ZnO can be used as a proper substitute of TiO_2 as the ETM layer without affecting the performance of PSCs significantly [89]. ZnO has material properties similar to that of TiO_2 [90], but it has some advantages over TiO_2: ability to be doped and higher electron mobility [36, 91].

The stability of perovskite devices with ZnO as ETL has been poor due to high carrier recombination and chemical interaction at the ZnO/perovskite interface, because the basic nature of ZnO may react with the organic cation (CH_3NH_3 +) in perovskite [38, 40, 41].

Properties of ZnO

ZnO is a II–VI compound semiconductor whose ionicity resides at the borderline between the covalent and ionic semiconductors [39], zinc oxide (ZnO) is n-type semiconductor, transparent metal oxide.it is the most prominent one due to its wide and direct bandgap (3.37 eV), extremely high transmittance in the visible region, exciton binding energy (63 meV), easy to etch, nontoxic, and low cost [92, 93]. Undoped and doped ZnO thin films are widely used in transparent

conducting layers because of their thermal stability [94]. The optical absorption coefficient value of ZnO thin films was relatively high (up to 5 x 10^4 cm^{-1}) [95]. Moreover, it can be easily solution-processed at low temperatures to yield structures with different morphologies [96].

ZnO is an important technological material, which can be doped to modulate structure and composition to cover a wide variety of optical and electronic properties, especially for application in solar cells. The dopants used for the ZnO films using group III elements B, Al, Ga and In, rare earth metals (group IIIB), group IV elements Si, Ge, and Sn. The dopants of ZnO for carrier concentration which range between (10^{16} to 10^{21}) cm^{-3} specific of experimental data, according to the method deposition. Figure 2.5 illustrates the various Carrier concentration of doped ZnO with different dopants [97-99].

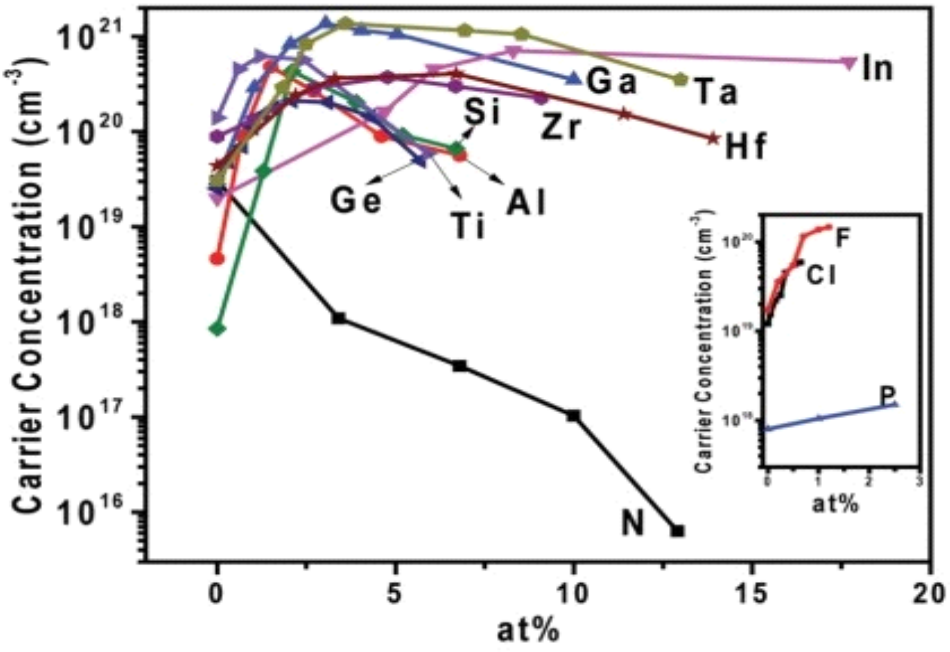

Figure 2.5: Doping ratios for different materials with carrier concentration [98].

2.5 Titanium oxide as electron transport layer

Background

The material most commonly used as the ETL is TiO_2, because Perovskite solar cells originated from previous dye-sensitized cells, and TiO_2 was used as mainly electron transport material (photoanode) [50, 100]. TiO_2 is one of the most extensively studied materials, and it is the ETL material most widely used by different research groups, the rising interest in its applications and

research in the last few years is due to its unique and outstanding structural, optical and electronic properties [101, 102]. TiO_2 exists in three crystalline phases: anatase, brookite and rutile, shown in Figure 2.6. The most widely used crystallographic structures (tetragonal) are anatase and rutile [100, 102]. TiO_2 thin films have been prepared by many techniques such as chemical vapor deposition, sputtering, sol–gel, pulsed laser deposition, plasma oxidation, oxidation of Ti metal, electron beam evaporation, and atomic layer deposition (ALD) [102, 103].

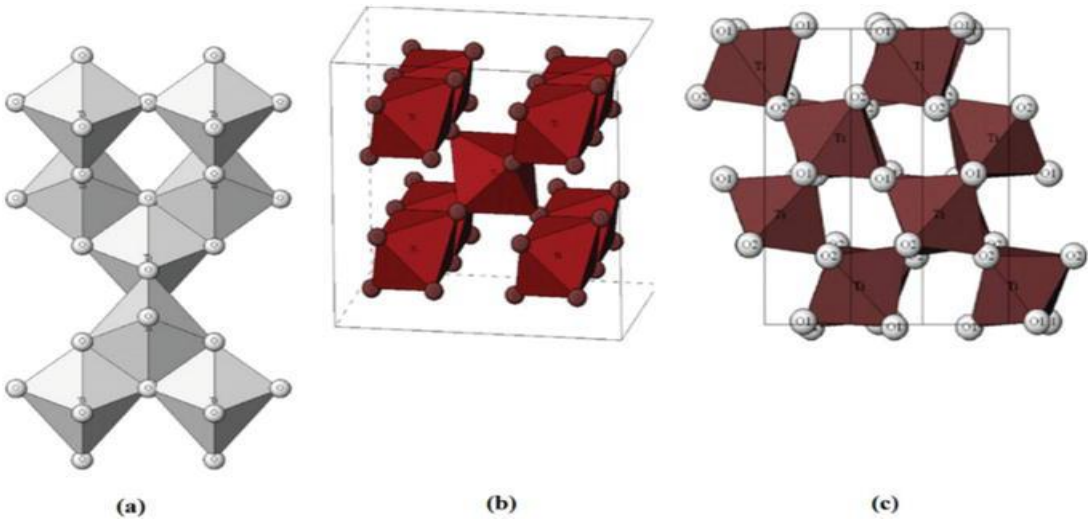

Figure 2.6: Crystalline structures of titanium dioxides (a) anatase, (b) rutile, (c) brookite [104].

2.6 Issues in Perovskite Solar Cells

2.6.1 The issue of stability

Although, all the exceptional optical and electronic properties of perovskite solar cells but a big challenge in the topic perovskite is the short-term and long-term stability. The degradation of PSC has been attributed to different factors (humidity, oxygen, temperature, and light). For describe these issues we will take methylammonium lead tri-iodide ($MAPbI_3$) is a proto-typical example of a known perovskite material [105-107].

- **Humidity and oxygen**

Humidity and oxygen will affect the chemical stability of perovskite solar cells, accompanied by the degradation of perovskite by changing the colour from dark brown to yellow [106].

The perovskite $MAPbI_3$ is a black material and can also exist in white or yellow phases [108]. Perovskites are unstable and highly degradable upon exposure to moisture of air because of the water solubility of their organic constituent. In this reaction pathway, a single water molecule is sufficient to degrade the perovskite material. But to dissolve the hydrogen iodide (HI) and $CH_3NH_2$by products, an excess of water is required. As a result of this reaction in a closed system, traces of water will partially decompose the hybrid perovskite until the HI has saturated the HI and H_2O or the vapor pressure of CH_3NH_2 has reached equilibrium. In exposure of sufficient water, the material can degrade completely to form PbI_2. One method used to solve this problem is the creation of a mixed halide perovskite [26, 105, 106, 109].

But this problem has been rectified by researchers as they have addressed that if perovskite films are prepared in an inert atmosphere using boxes filled with nitrogen or argon then this problem can be overcome. Further this step is followed by the immediately encapsulating the whole device in an air tight sealant having the same inert gases [105, 110, 111].

- **Temperature**

Thermal stability in normal practical condition, exposure of PSC to sunlight will increase temperature of solar panel. The accumulation of heat can get a temperature as high as 85°C. There are two kind of thermal degradation in PSC: one is the intrinsic thermal instability of the perovskite material and another comes from another unstable layer such as HTM [106, 109].

The degradation can result from the intrinsic thermodynamic instability of the perovskite crystal structure. Perovskite materials have different phases depending on their temperature [109, 112]. At around 55°C $MAPbI_3$ experiences a phase transition from a tetragonal crystal structure into a cubic one which decreases the cell performance. The decomposition of $MAPbI_3$ into PbI_2 and CH_3NH_3I is exothermic, implying that the tetragonal structure is thermodynamically unstable at room temperature regardless of outside factors such as moisture or oxygen [105, 108, 113].

It has also been shown that perovskites exhibit similar degrading behavior in both air and vacuum, suggesting that the degradation mechanism may indeed be intrinsic and independent of environmental factors. It should also be remembered that the stability of each individual layer affects the stability of the whole cell [106, 114].

- **Photo Stability**

The instability of the perovskite material include illumination, interaction with ETL and HTL materials. The degradation of perovskites by UV light could be originated at the TiO_2 layer. In

UV light the lead-halide parts of perovskites may decompose and form metallic lead Under illumination, any excess PbI_2 in the perovskite layer can also result a faster degradation of the cell in an ambient atmosphere than that of cells with no excess PbI_2 [22, 115, 116].

It has been proposed the degradation mechanism which is related to the surface chemistry of TiO_2, as shown in Figure 2.7. Many oxygen vacancies are existence in the TiO_2, especially at the surface, which can adsorb molecule oxygen in ambient atmosphere to form charge transfer complex (O_2^-–Ti_4^+) (Figure 2.7.a). The excited electron–hole pair is generated on TiO_2 upon UV light exposure. The hole in the valence band can recombine with the electron at the oxygen adsorption site, thus leading to the release of the absorbed oxygen. Then a free electron is left in the conduction band. Meanwhile, the unfilled oxygen vacancy site, which served as deep surface traps site, is left on the TiO_2 surface (Figure 2.7.b) and (Figure 2.7.c). These remaining electrons will recombine with the excess holes in the p-doped transfer layer (Figure 2.7.d). As the increase of recombination of electrons and holes and trap sites, the device performance will be influenced [105].

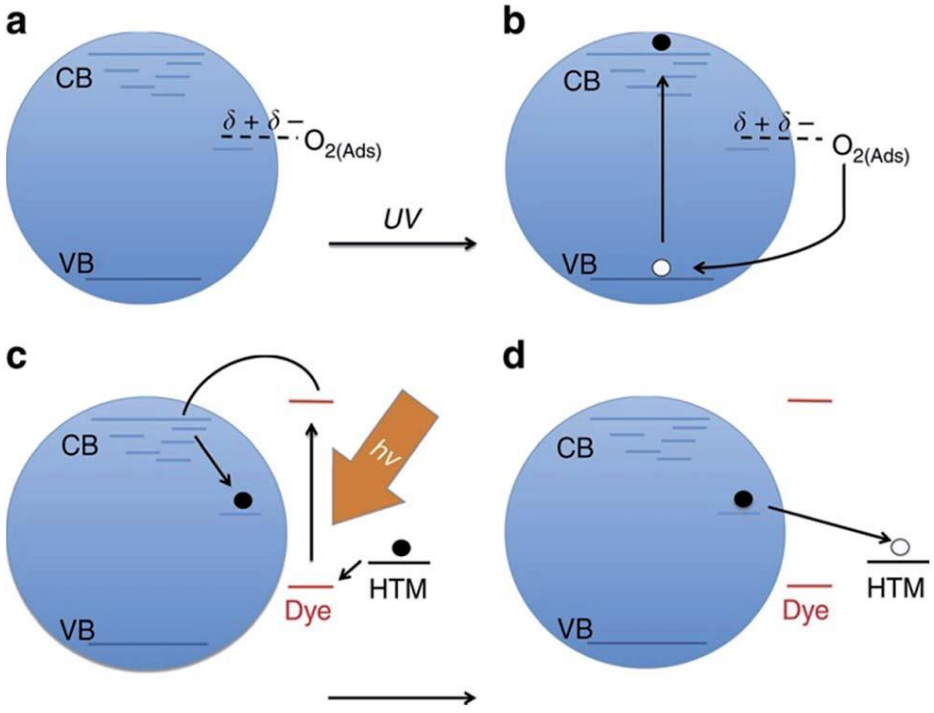

Figure 2.7: Schematic diagram of proposed degradation mechanism upon UV-light irradiation [105].

2.6.2 Ions migration

Organic–inorganic perovskite solar cells, consisting of a polycrystalline perovskite active layer sandwiched between electrodes, Perovskite is well known to be an ionic conductor. Perovskite can easily decompose and generate ions, these generated ions can migrate [117, 118].

The ion migration, proposed to be responsible for the formation of an internal field within the planar device with symmetric contacts, is observable not only under light illumination but also in the dark under polarization [119-121].

Before the ion migration process positive charged cations and negative charged anions are anions are uniformly distributed inside bulk perovskite. With influence of the internal electric field, the cations drift towards the interface between perovskite-hole transport (p-type) layer and anions drift towards perovskite-electron transport (n-type) layer. These ions change the internal electric field profile inside bulk perovskite and changes, the IV characteristics of the solar cell. MA cations and iodine anions have lowest activation energy for migration and thus, it is easier for these two ions to move compared to other ions. From formation energy and activation energy calculations, it can be interpreted that MA cations and I anions are most dominant species in ion migration process inside bulk perovskite. When bias is applied across the device depending on the biasing direction ions can either accumulate towards the interfaces or migrate back towards the bulk. Thus, the internal electric field inside the material also changes. This change in internal electric is responsible for switchable photovoltaic behaviour. Which results in the occurrence of the well-known hysteresis in the current density–voltage curves of PSCs [69, 113, 119].

2.6.3 Toxicity issue

Along with cell stability, one of the most commonly used material in perovskite based solar cells is lead, which is toxic in nature and overall environmental impact of perovskite solar cells, as well as the disposal and recycling of cells at the end of their service life. In fact that lead has been a major constituent of nearly all highly efficient perovskite cells to date [122, 123].

Perovskite gets easily degraded when it is exposed to environment where it comes in contact with humidity and the ultra violet radiations. Lead can leach out from the panel of solar cell panel into the surroundings into the environment and can cause various ecological and health related challenges [124].

The research now a days is basically focused to increase the use of these devices by focusing on their addressing the toxicity and degradation issues related to them, in order to realistically produce portable PSC devices with the current legislation, either the lead content had to fall under the limit, or it had to be completely replaced. For this very problem an environmentally friendly and benign element like tin has been into the proposition as an alternate source to lead based perovskites. The tin cousins of MAPI, namely MASnI3, and CsSnI3 have shown a rather high potential for PV applications, but they present an extreme sensitivity to oxygen. A good encapsulation can be the solution to this issue [122, 125].

Additionally, the solvents used in the fabrication of PSCs (dimethylformamide or DMF and dimethylsulfoxide or DMSO) should be taken into account. These solvents are miscible with water, and thus, it is sensitive to the absorption through dermal contact and ingestion [122, 126].

Chapter 3

Numerical simulation, results and discussion

3.1 Introduction

In this work, we have implemented the simulation of ETL/CH3NH3PbI3/CuSCN perovskite solar cell, with two electron transport materials. Numerical simulation is carried out using the softwareSCAPC-1D (Solar Cell Capacitance Simulator). We studied the role of both ZnO and TiO_2 as an electron transport material ETM. To discover its effects on perovskite solar cell parameters (Jsc, Voc, FF, and efficiency).

3.2 SCAPS-1D modelling

SCAPS (Solar Cell Capacitance Simulator) is a one dimensional solar cell simulation program developed by university of Gent, Belgium. It has been applied to the study of different types of solar cells such as CZTS, CIGS… etc. and it can be used to simulate PSC [127, 128]. Compared with other software, SCAPS has a very intuitive operation window and diversified models for grading, defects and recombination [129]. Once all parameters defined, it behaves like a real-life counterpart [130]. The main features of SCAPS including materials and defects properties can be defined in 7 semiconductor layers. This software is designed to simulate and helps us to analyse the $J{-}V$characteristics curve, ac characteristics ($C{-}V$ and $C{-}f$), spectral response (QE) of a device, power conversion efficiency (PCE), fill factor (FF), short-circuit current (Jsc), open circuit voltage (Voc), energy bands of materials used in solar cell and concentration of different material used by solving the semiconductor basic equations [36, 127].

3.2.1 Basic Equations

The SCAPS software numerically solves the basic equations of semiconductors, including Poisson's equation, transport equation, and continuity equation for electrons and holes [131].

Poisson's Equation

Poisson's equation is used to describe the relationship between potential and space charges.

$$\frac{\partial^2 \varphi}{\partial x^2} = \frac{q}{\varepsilon}\left[n(x) - p(x) - N_D^+(x) + N_A^-(x) - p_{t(x)+n_t}(x)\right] \quad (3.1)$$

where, φ is the potential, q is the elementary charge, $\varepsilon$is the permittivity, n is the density of free electron, p is the density of free hole, N_D^+ is the ionised donor-like doping density, $N_A^-$is the ionised acceptor-like doping density, p_t is the trapped hole density , n_t is the trapped electron density.

Continuity equations

It is called governing equation because drift, diffusion, generation, and recombination are analysed simultaneously [127]. Equation (3.2) and equation (3.3) represent continuity equation for concentration change in electron and hole.

$$\frac{\partial n}{\partial t} = \frac{1}{q}\frac{\partial J_n}{\partial x} + (G_n - R_n) \quad (3.2)$$

$$\frac{\partial p}{\partial t} = \frac{1}{q}\frac{\partial J_p}{\partial x} + \left(G_p - R_p\right) \quad (3.3)$$

Where, $G_n(G_p)$ is the electron (hole) optical generation rate, $R_n(R_p)$ is the electron (hole) recombination rate, J_n, J_p are the electron and hole current densities given by Transport equations (3.4) and (3.5).

$$J_n = nq\mu_n E + qD_n\frac{\partial n}{\partial x} \quad (3.4)$$

$$J_p = pq\mu_p E - qD_p\frac{\partial p}{\partial x} \quad (3.5)$$

q is the elementary charge, $\mu_{n(p)}$ is electron (hole) mobility, and $D_{n(p)}$is diffusion coefficient of electrons (holes) and from Einstein relationship, the diffusion coefficient is depended upon the mobility of carrier with the product of carrier lifetime. Relation of D_n and D_p is show in equation (3.6) and (3.7).

$$D_n = \frac{\mu_n k_B T}{q} \quad (3.6)$$

$$D_p = \frac{\mu_p k_B T}{q} \tag{3.7}$$

Where, k_B is Boltzmann constant, T is temperature.

Diffusion Length

Diffusion length describes the transport ability of carriers in a solar cell device. It depends on diffusion coefficient and carrier lifetime [127]. That is represented in equations (3.8) and (3.9).

$$L_n = \sqrt{D_n \tau_n} \tag{3.8}$$

$$L_P = \sqrt{D_P \tau_P} \tag{3.9}$$

Where, $L_{n(p)}$ is electron (hole) diffusion length, $\tau_{n(p)}$is electron (hole) lifetime.

3.2.2 SCAPS program interface

SCAPS-1D simulation start-up panel interface is called action panel is the main window in SCAPS (Figure 3.1), in this panel all the external parameters of simulation can be controlled (such as temperature, voltage, frequency, solar light…etc).

The action panel can be divided into six parts or sections which can be described as following:

1) Section (A) "Set problem" is dedicated to define the problem of the structure, the materials, and all the physical properties of the simulated solar cell.
2) Section (B) represented in "Action" where the external electrical conditions can be controlled. Such as the applied bias starting point, step and final voltage, the frequency…etc.
3) Section (c) represented in "Illumination" which is dedicated for the selection of light and dark condition and the type of spectrum for simulation.
4) Section (D) is the "Working point" for specify the working point of temperature values, in addition to the specification of series or shunt resistances if they are required.
5) Section (E) represented by "calculate" which can start the calculation process of simulated device.
6) Section (F) represented by "Result of calculations" with the role of Displaying curves and results of simulated device.

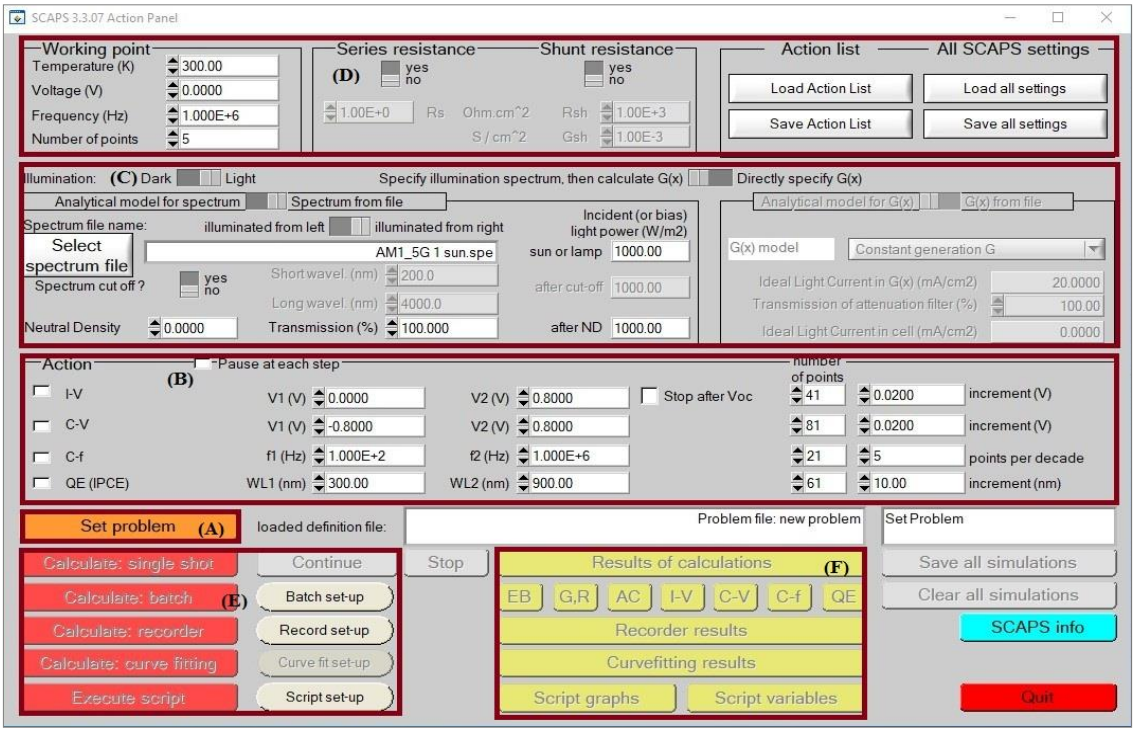

Figure 3.1: SCAPS − 1D simulator start-up panel interface.

3.2.3 Solar cell structure Definition

To define the problem, thus the geometry, the materials and all properties of the solar cell, we click on "Set problem" button on the action panel**,** a new window is opened which is the solar cell definition panel (Figure 3.2). This interface plays a significant role in device simulation, in this panel we can create different layers and define their physical parameters and properties, we can also have a visualization of the device structure.

There are three parts of device definition interface and details in this panel:

- Section (1), in this part we can define structures consisting of up to 9 layers. The first layer is the back contact; the last one is the front contact. The user can specify the properties of all layers.
- Section (2) is a display of defined photovoltaic device structure with back and front contact. There are also additional buttons for the selection of the device illumination either from back contact side or front contact side, the direction of the voltage applied to a device and finally a button dedicated to invert the structure layers order.

- Section (3) has buttons for saving definition file in SCAPS library or an external library, loading of previously saved device structure definition files. Cancel and OK buttons are for leaving or entering device definition interface and return to the start-up interface.

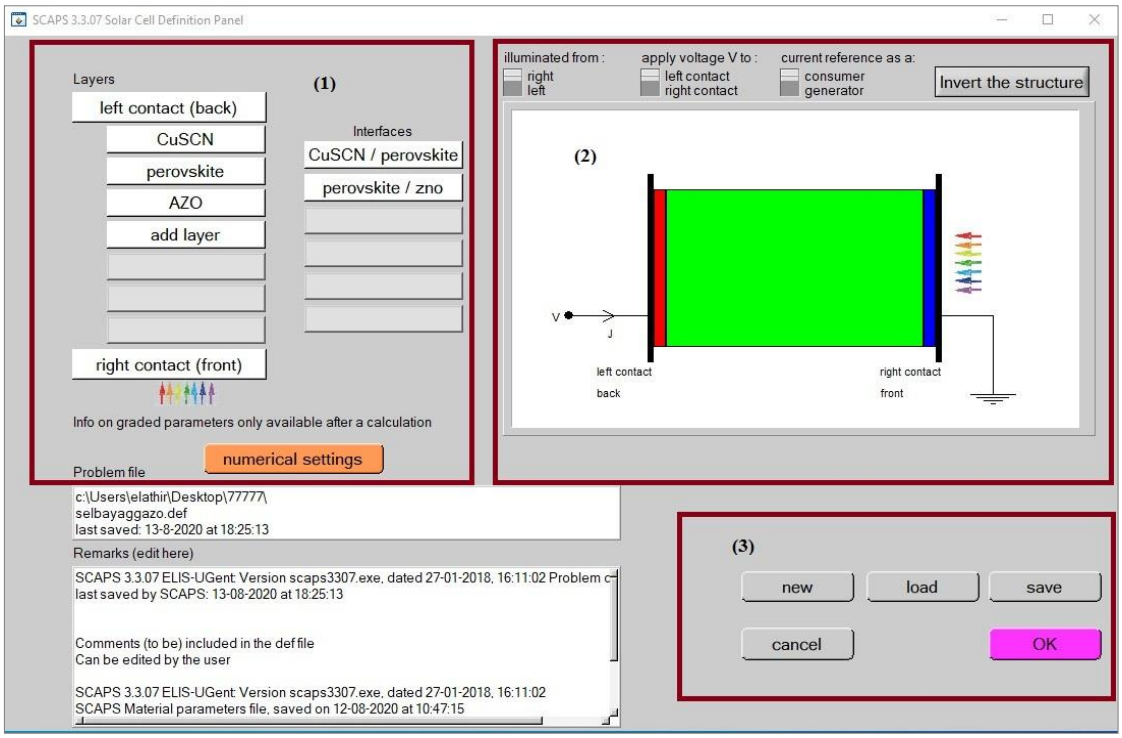

Figure 3.2: Device definition interface

3.2.4 structure layers properties

We can define or add layers in SCAPS-1D program by clicking on the button “add layer” given in section 1 of (Figure 3.2) therefore, a new window will popup called “layer properties panel” (Figure 3.3).

The layer properties panel can be divided into three main parts as following:

- Section (1): to set or add the layer physical parameter values in layer properties interface.
- Section (2): the definition of the material defects parameter by pressing the button “Add Defect”.
- Section (3): defining the absorption factor for the substance. This factor can be defined either from internal calculation model or from file.
- Section (4): has buttons for saving the definition of the material file in SCAPS library and loading files of material definition previously saved. Cancel and OK buttons are for leaving the layer properties panel and return to the solar cell definition panel.

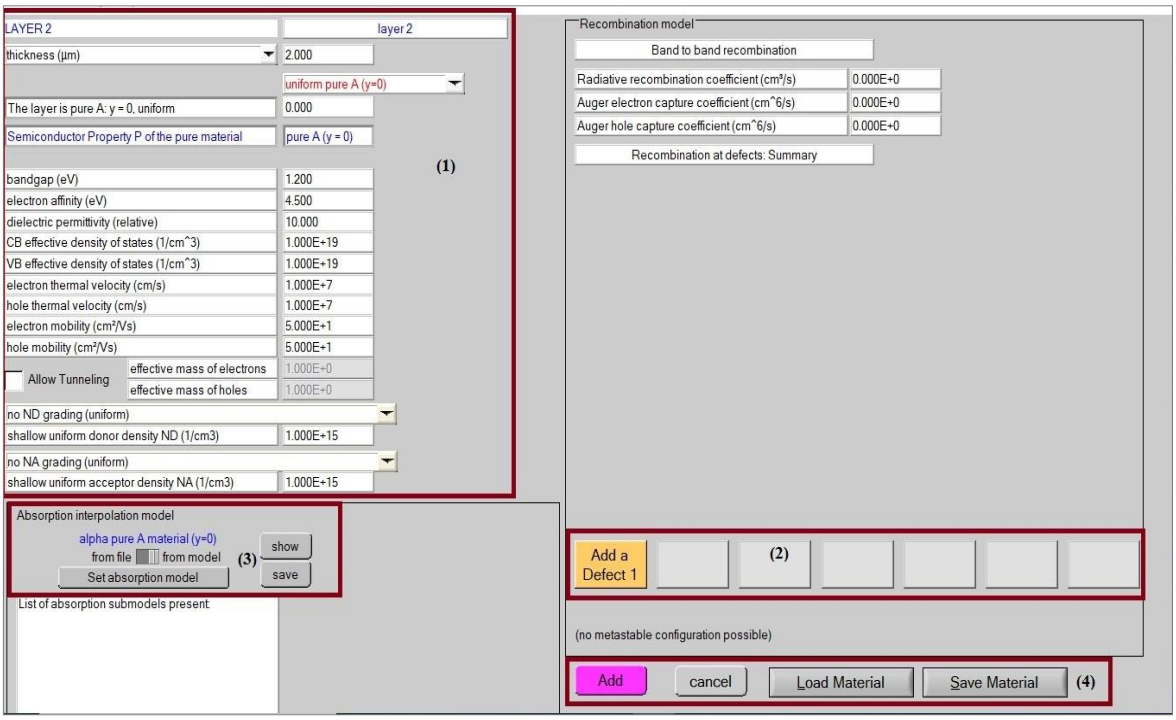

Figure 3.3: Layer properties panel.

3.2.5 Calculate and display the simulated curves

After introducing all the necessary data (configuration of the solar cell, layer properties, and material properties), the button “calculate” in the action panel interface can be clicked to start the simulation. Therefore, the Energy Bands Panel opens, and calculations begin (see Figure 3.4). In this window we can obtain the results curves. We select for example the (I-V) button in the energy band panel window we can obtain the (I-V) curve (see Figure 3.5). Do the same for the rest the curves (C-V), (QE), (gen-rec) …etc.

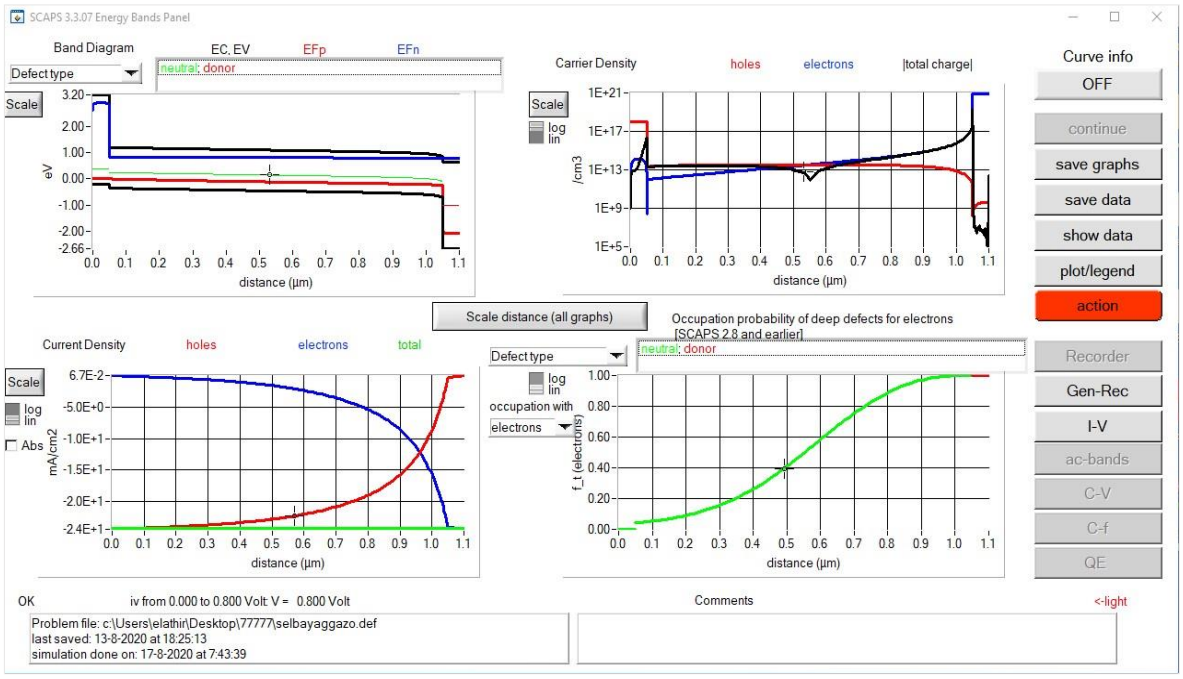

Figure 3.4: Energy Band-s Panel

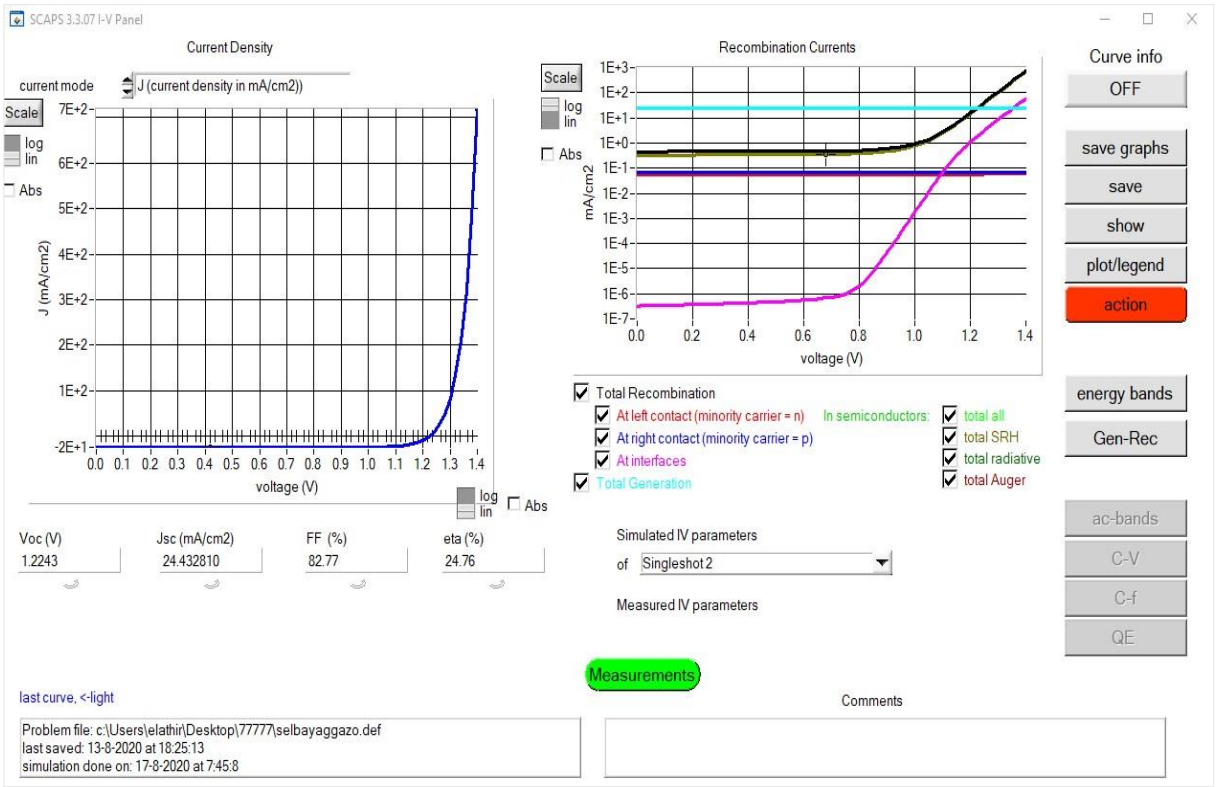

Figure 3.5: I-V curve obtained using SCAPS simulator

3.3 Results and discussion

3.3.1 Structure simulation

The simulation of lead-based perovskite solar cell is based on the n-i-p planar (Figure 3.6) which can be simulated using any thin-film simulator and therefore considered similar to the structure of thin film semiconductor based solar cell. Electrical characteristics of a perovskite cell are analyzed by simulating the device in SCAPS-1D software. In this study, zinc oxide (ZnO) and titanium oxide (TiO_2) are used as an electron-transport material, $CH_3NH_3PbI_3$ as an active layer (also called the absorber layer), and copper thiocyanate (CuSCN) as a hole-transport material. The simulations were performed under the Standard Test Condition (STC) AM1.5G, 1000 W/m2, and T=300 K.

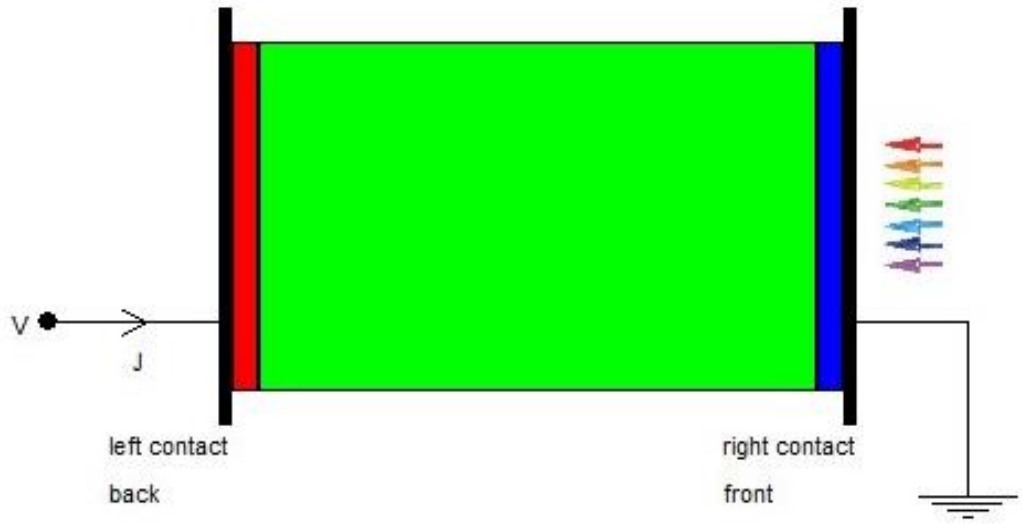

Figure 3.6: Perovskite solar cell structure used in this study.

In order to simulate this type of solar cell a lot of parameters must be provided about device structure, materials, and physical properties to fine tune the simulation (band gap energy, electron affinity, relative permittivity, hole mobility, electron mobility, valence band effective density of states, conduction band effective density of states, acceptor and donor densities doping, and defect density). The obligatory physical input parameters show in (Table 3.1).

Table 3.1: Properties of the used materials for the simulation.

Parameter	TiO_2 (ETL)	ZnO (ETL)	$CH_3NH3PbI3$ (Absorber)	CuSCN (HTL)
Thickness, d(μm)	0.05	0.05	1	0.05
Band gap, Eg(eV)	3.2	3.3	1.55	3.4
Affinity, χ (eV)	3.9	4.1	3.9	1.9
Permittivity, εr	9	9	6.5	10
Effective density of states at CB, Nc (cm^{-3})	1×10^{21}	4×10^{18}	2.2×10^{18}	1.7×10^{19}
Effective density of states at VB, Nv (cm^{-3})	2×10^{20}	1×10^{19}	1.8×10^{19}	2.5×10^{21}
Electron mobility, μn (cm^2/Vs)	20	100	2	1×10^{-4}
Hole mobility, μp (cm^2/V s)	10	25	2	1×10^{-1}
Donor concentration, Nd (cm^{-3})	1×10^{19}	1×10^{18}	5.21×10^{9}	0.0
Acceptor concentration, Na(cm^{-3})	1.0	1×10^{5}	5.21×10^{9}	1×10^{18}
Defect properties				
Density of defects, Nt (cm^{-3})	1×10^{15}	2×10^{17}	2.5×10^{13}	1×10^{14}
Capture cross section for electrons, σ_n(cm^2)	SCAPS	1×10^{15}	SCAPS	SCAPS
Capture cross section for holes, σ_p(cm^2)	SCAPS	1×10^{15}	SCAPS	SCAPS

3.3.2 Eefect of Zno as electron transport layer

3.3.2.1 Effect of ZnO thickness on solar cell

The electron transport layer thickness is one of the parameters that may have an important role to determine the performance of PSC. The effect of ZnO layer thickness on the PV parameters was calculated and it is varied from 10 nm to 100 nm, the results are shown in Figure 3.7. Although the increase in the ZnO layer thickness, the value of open circuit voltage (Voc) and fill factor (FF)

remained unchanged. On the other hand, the short circuit current density (Jsc) and power conversion efficiency (PCE) are dropped with the increase of ETL thickness.

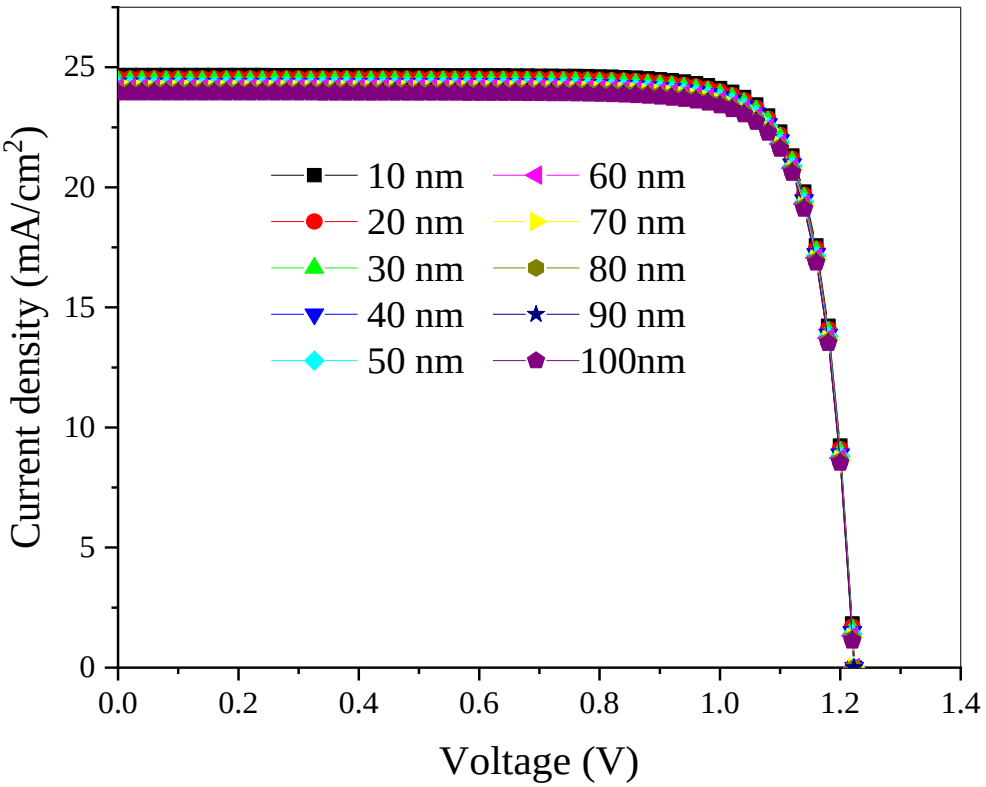

Figure 3.7: Effect of change thickness of ETL on the J-V characteristics.

Figure 3.8 shows the output parameters *Jsc*, *Voc*, FF and PCE of the solar cell versus increase in the thickness. The value of (Voc), (FF) remained unchanged. But the short circuit current density (Jsc) and (PCE) are dropped, (Jsc) decreases from 24.67 mA/cm2 to 23.94 mA/cm2, PCE decreases from 24.87% to 24.09% with the increase in ETL thickness.

Firstly, we can explain the stability in FF; FF expresses the quality of the solar cell and it is related to properties of active layer. For the Voc the stability is due to the unchanged band gap of the perovskite layer because Voc is related to Eg. Secondly, the drop in the Jsc is due to the increase of light absorption in the ZnO layer with the increase of its thickness. Which affect the number of transmitted photons to the active layer (Perovskite in this case), and hence results a decrease in the photo generated carriers in these layers, more evidence can be concluded by analyzing the quantum efficiency curve (Figure 3.9).

As zinc oxide thickness increases, the quantum efficiency decreases at short wavelengths (300-400 nm). It is known that the short wavelengths are absorbed near the surface of the solar cell and are far from the effective region (see Figure 1.5), this leads to a loss in the effective

generated carriers and thus a decrease in the short circuit current. Where there is a direct proportionality between the quantum efficiency and short circuit current density (show in equation (1.4)). Finally, the power conversion efficiency (PCE) of solar cell decreases by the drop of the Jsc.

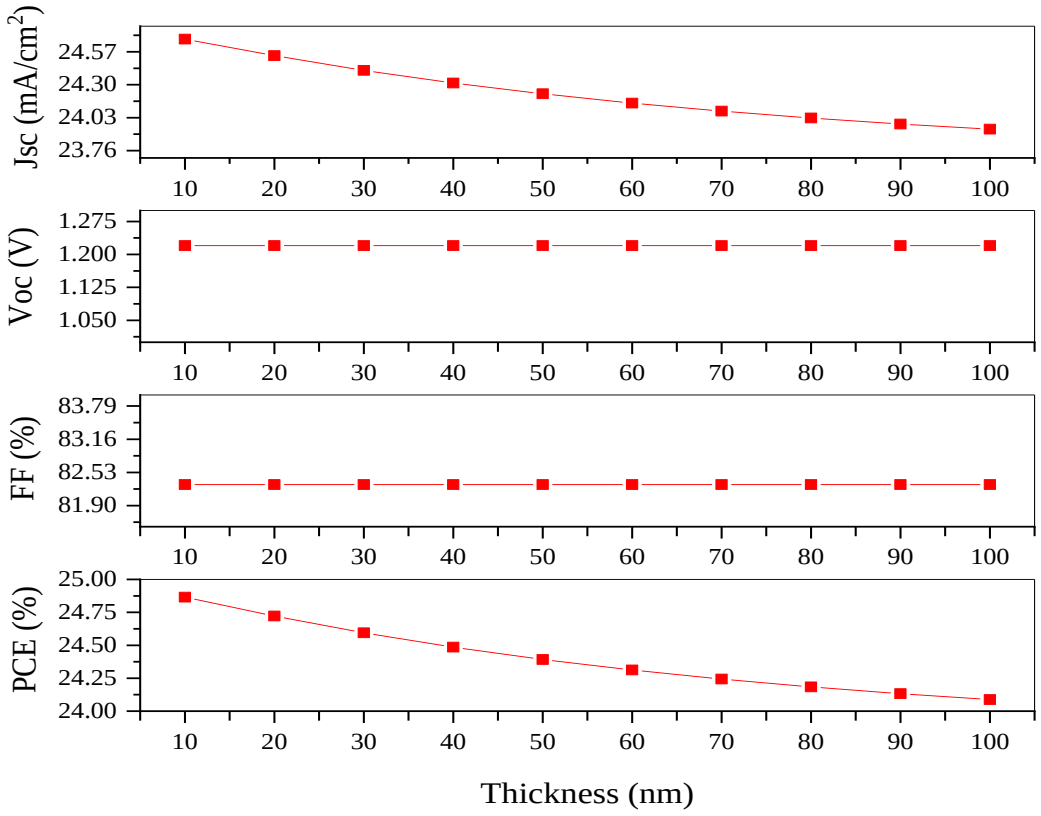

Figure 3.8: Influence of ZnO thickness on the solar cell performance.

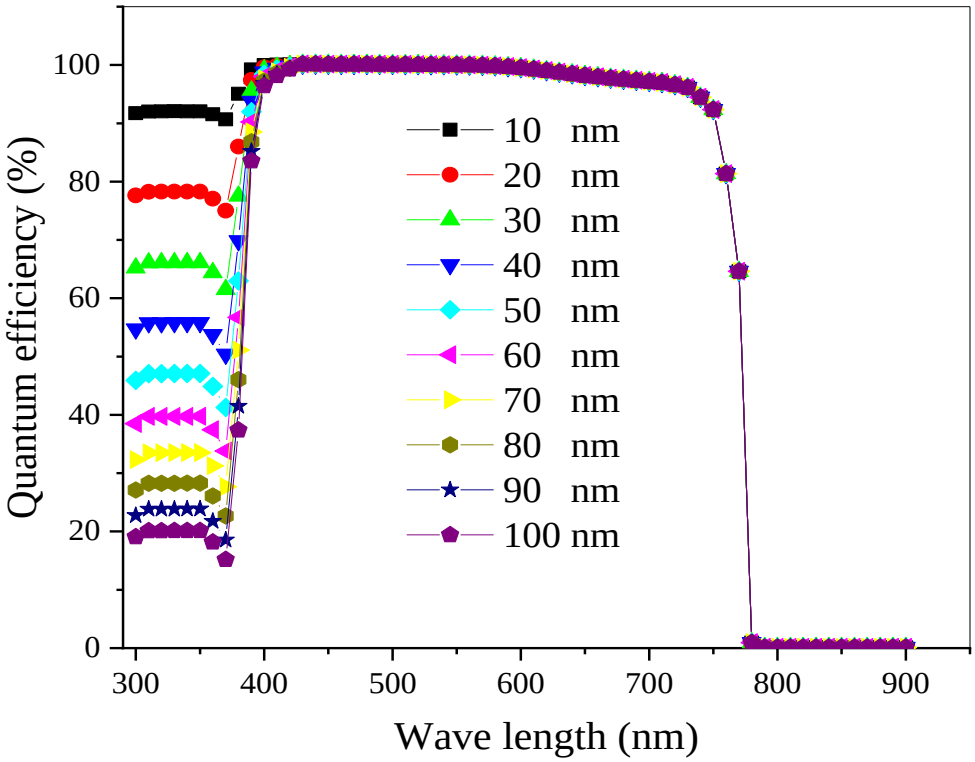

Figure 3.9: Quantum efficiency of perovskite solar cell with change thickness of ETL.

3.3.2.2 Effect of doping concentration on performance of solar cell

The effect of ZnO layer doping on the PV parameters was calculated and it is varied from $1\times10^{+16}$ cm^{-3} to $1\times10^{+21}$ cm^{-3}. Where the thickness of ZnO is fixed at 30 nm, the results are shown in Figure 3.10. The curves show that the increase in the ZnO layer doping concentration has different effects on the PV parameters: the value of Voc remained unchanged at 1.22 V. While there is very small decrease in Jsc which can be neglected. On the other hand, there is a relative remarkable increase in FF from 81.96% to 82.8% and power conversion efficiency from 24.45% to 24.75%.

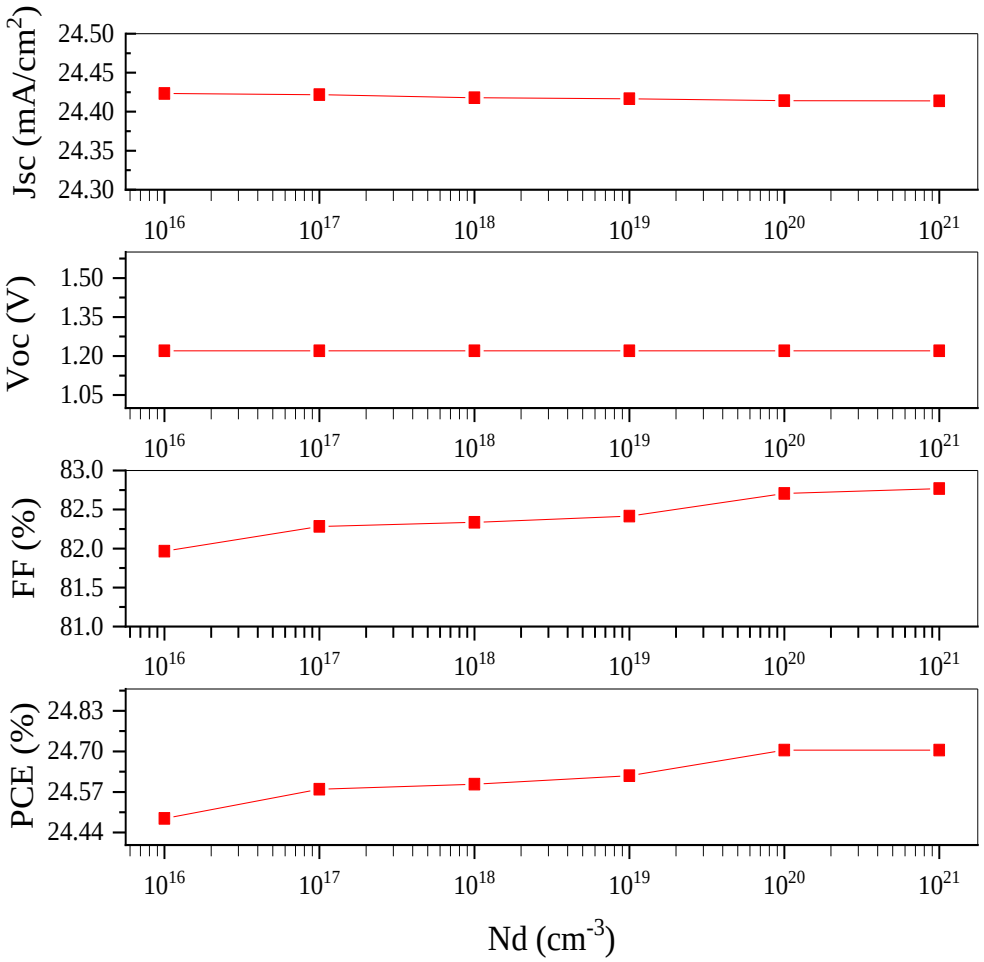

Figure 3.10: Influence of ZnO doping concentration on the solar cell performance.

The increase in PCE is mainly due to the increase in FF, as the doping concentration increases. that means the conductivity value increases and the Resistivity (R_s) decreases, which greatly affects the fill factor of the solar cell. Voc remains unchanged and independent of doping concentration in electron transport layer. Also, the open circuit voltage depends on the properties of the active layer.

3.3.2.3 Effect of ZnO defects on the performance of solar cell

We studied the effect of ETL (zinc oxide) defects on performance of perovskite solar cell, where the concentration of these defects changed from 1×10^{14} cm^{-3} to 1×10^{18} cm^{-3}, taking into account the thickness of electron transport layer of 30 nm. Simulation results are shown in Figure 3.11. When increasing the defects density in the electron transport layer, we observe the stability of both open circuit voltage at the value 1.22 volt and fill factor at the value 82.33%, With a decrease in PCE from 24.88% to 24.56%, this is mainly due to the decrease in the short circuit current. The

decrease in the short-circuit current can be explained by the recombination in the active region extending in electron transport layer. As the defect density increases, the probability of capturing the photo-generated carriers at the surface (short wavelengths) increases, and thus a decrease in the photocurrent density, and this is evident in Figure 3.12. This can also be explained by the presence of series resistance R_s.

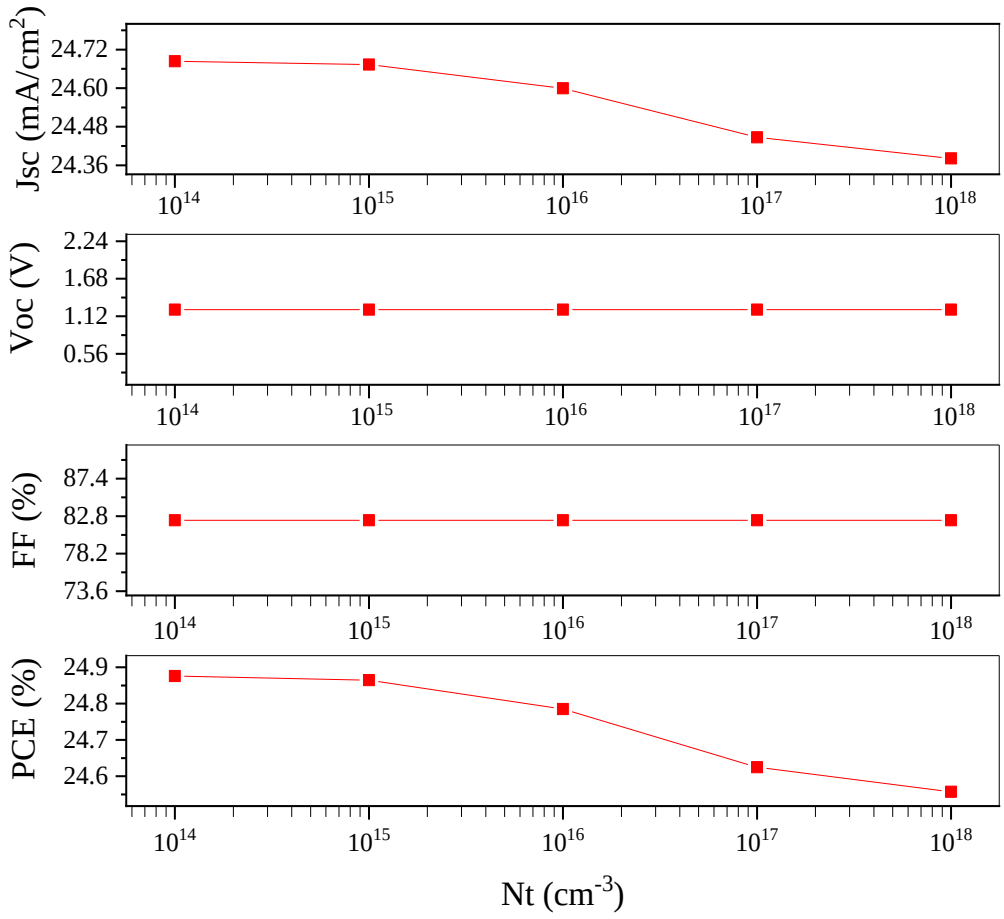

Figure 3.11: Influence of ZnO defect density on the solar cell performance.

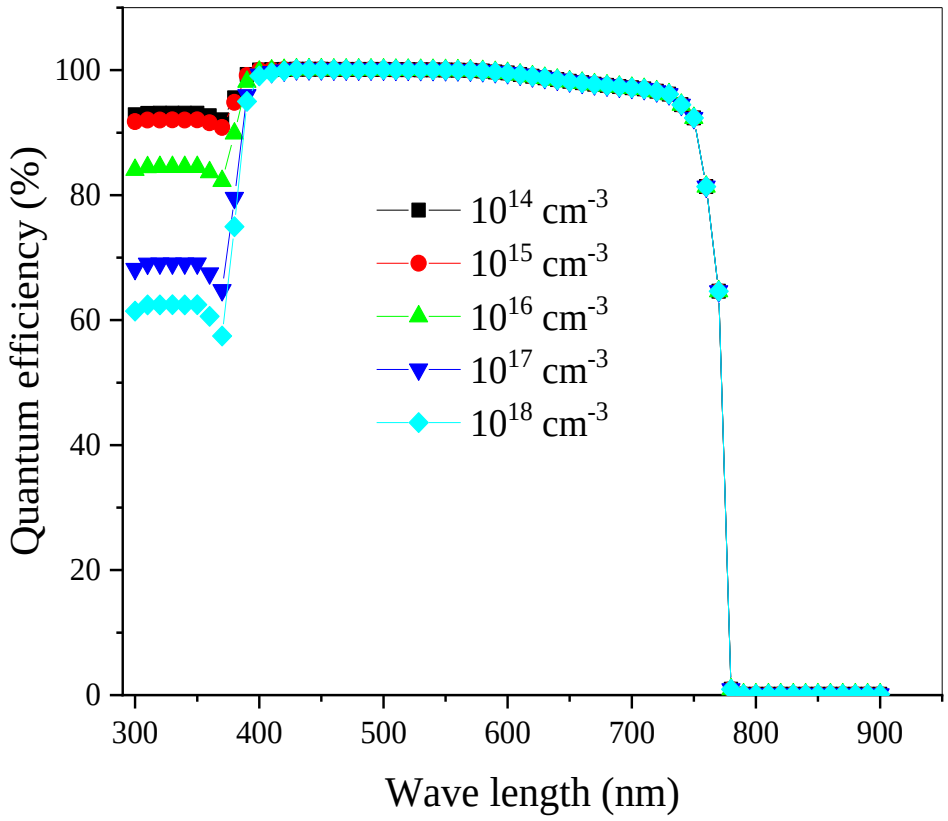

Figure 3.12: Quantum efficiency of perovskite solar cell with change ZnO defect density.

3.3.2.4 Effect of interface trap density ZnO/perovskite

Figure 3.13 shows the effect of changing the interface trap density on the J-V characteristics, as the thickness of the electron transport layer was fixed at 30 nm. With changing the density of these traps from1×10^{8} cm^{2} to 1×10^{15} cm^{-2}.

The simulation results showed the effect of trap density on the output parameters of the solar cell, shown in Figure 3.14. At low densities (less than 1×10^{11} cm^{-2}), the effect was almost negligible, but at high densities, the deterioration becomes evident. We notice a degradation in open circuit voltage starting from 1×10^{11} cm^{-2}, this is due to the presence of shunt resistance, where with increasing the traps density, the shunt resistance decreases. Low shunt resistance causes power losses in solar cells by providing an alternate current path for the photo-generated current. Such a diversion reduces the amount of current flowing through the solar cell junction and reduces the voltage from the solar cell, and This directly affected the PCE, as it decreased from 24.60% to 17.13%. Also, the trap density had no significant effect on the short circuit current density, Where decreasing from 24.42 mA/cm2 to 24.18 mA/cm^{2}, and the same for the fill factor, as it decreased

to the value 69.65%, with strange behaviour at Densities 10^{11} cm^2 and 10^{12} cm^2 where we notice an increase in FF, and this could be due to the shunt resistance R_{sh} and the ideality factor η.

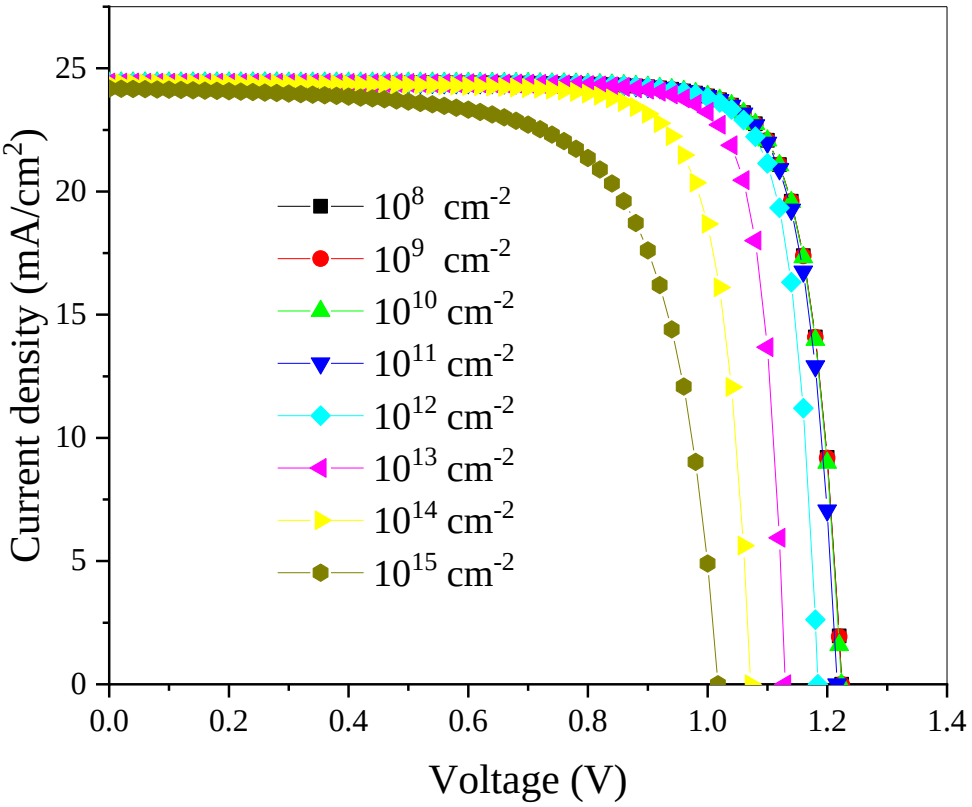

Figure 3.13: Effect of change interface traps density ZnO/perovskite on the J-V characteristics.

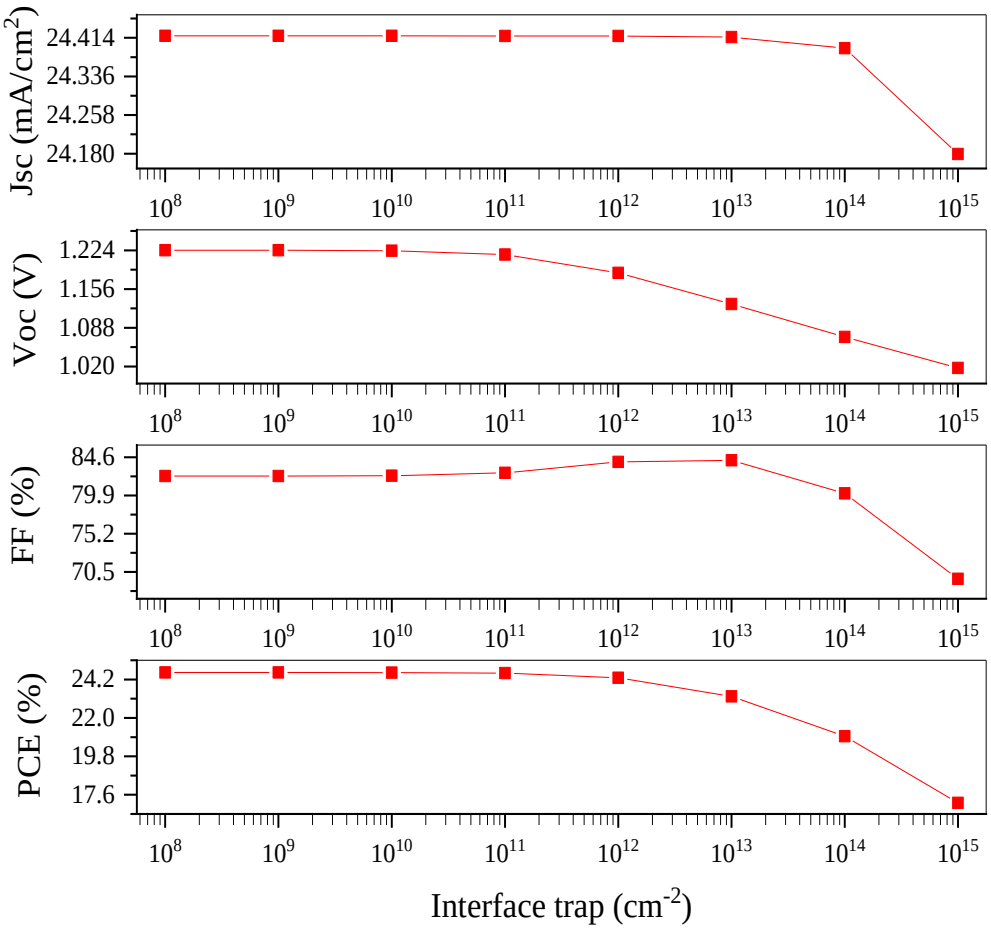

Figure 3.14: Influence of interface trap density on the solar cell performance.

3.3.3 Eefect of TiO_2 as electron transport layer

3.3.3.1 Effect of TiO_2 thickness on solar cell

The effect of electron transport layer increasing thickness on the PV parameters was calculated by changing the thickness of TiO_2 from 1nm to 100 nm. The simulated (J-V) characteristics are shown in Figure 3.15. Although the increase in TiO_2 layer thickness we observe constancy in Voc a value 1.22 V. On the other hand, there is a decrease in Jsc from 24.74 to 24.56 mA/cm^2.

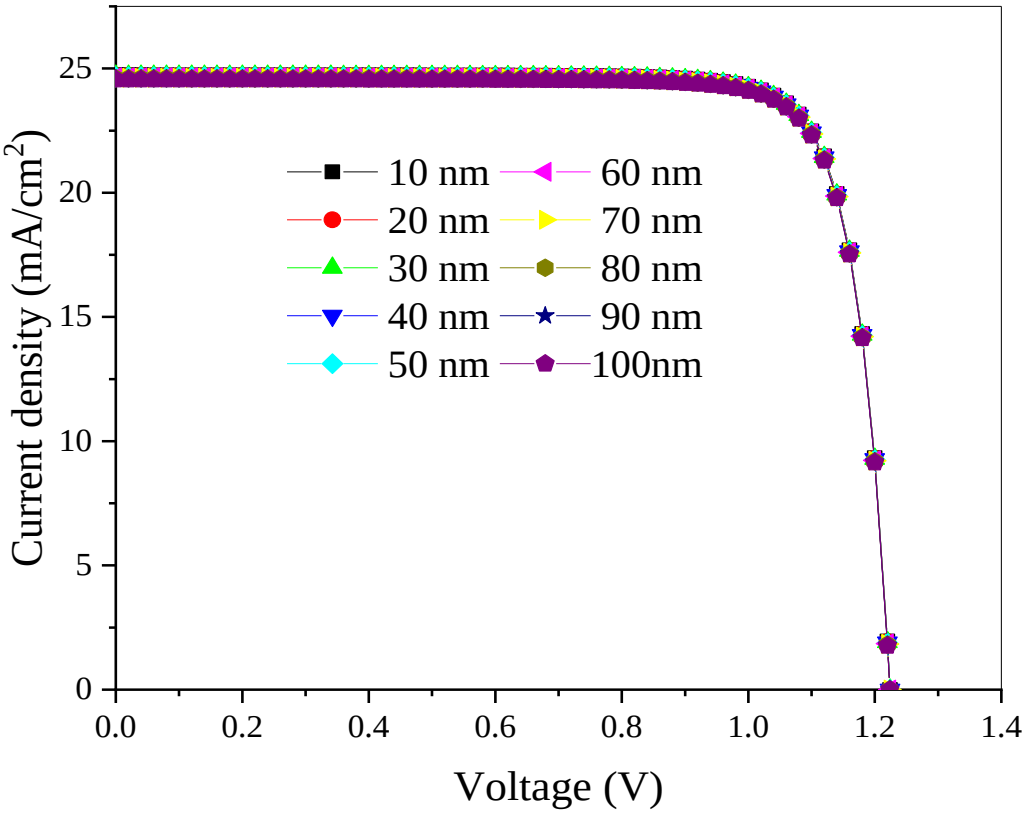

Figure 3.15: Effect of TiO_2 thickness on the J-V characteristics.

The evaluated parameters of simulation results *Jsc*, *Voc*, FF and PSC, versus increase in the thickness are shown in Figure 3.16. We observe with increasing thickness, there is a decrease in Jsc from 24.74 to 24.55 mA/cm^2 and power conversion efficiency (PCE) from 25.04 to 24.85%. On the other hand, the open circuit voltage (Voc) maintains the same value at Voc a value 1.22 V. The Fill factor (FF) are also constant at the value 1.22 V.

The drop in the Jsc is due to the increase of light absorption in the TiO_2 layer with the increase of its thickness. Which affect the number of transmitted photons to the active layer (Perovskite in this case), and hence results a decrease in the photo generated carriers in this layer, more evidence can be concluded by analyzing the quantum efficiency curve in Figure 3.17. We observe the quantum efficiency decreases at short wavelengths (300-400 nm). Where they are absorbed near the surface of the solar cell and are far from the effective region, this leads to a loss in the effective generated carriers. Thus, a decrease in the short circuit current, with titanium oxide layer thickness increases. The conversion efficiency "PCE" of solar cell decreases by the drop of the Jsc.

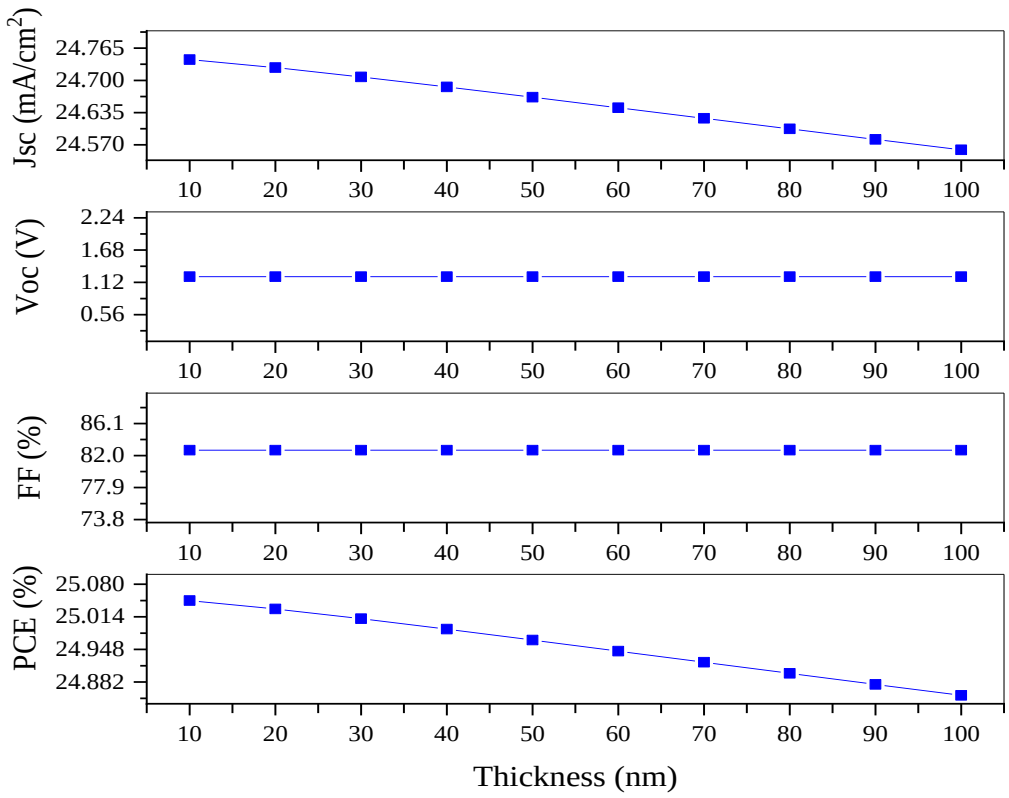

Figure 3.16: Influence of TiO_2 thickness on the solar cell performance.

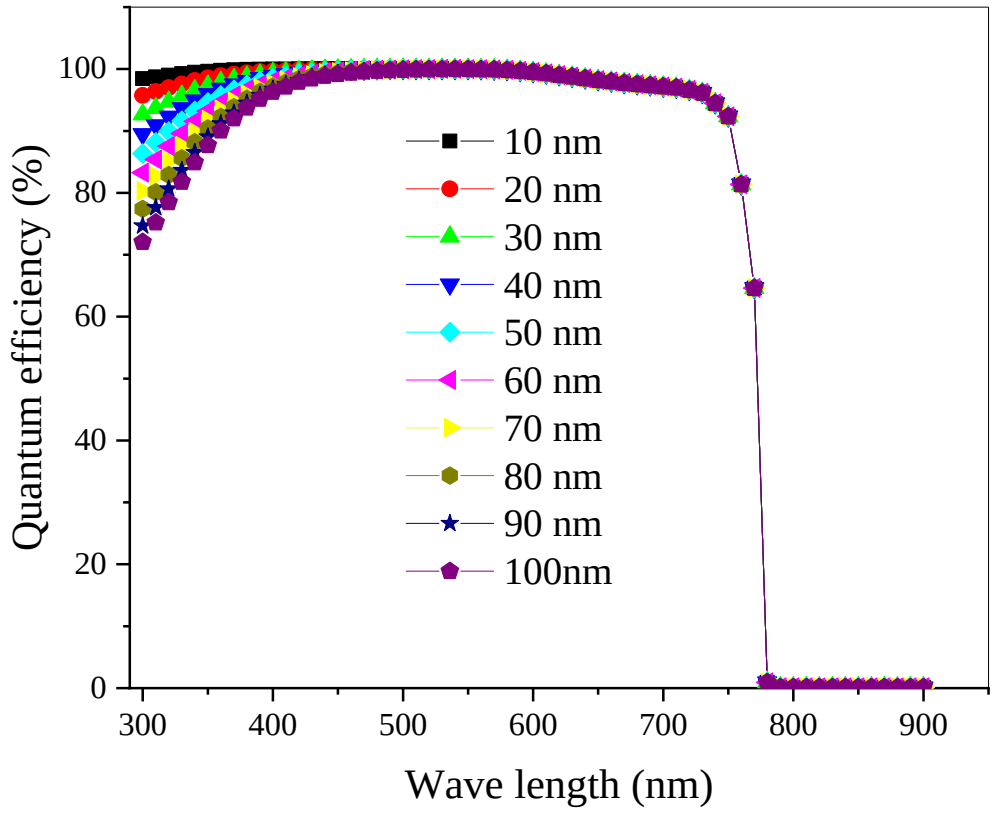

Figure 3.17: TiO_2 thickness effect on quantum efficiency of perovskite solar cell.

3.3.3.2 Effect of TiO_2 doping concentration on performance of solar cell

The effect of electron transport material (oxide titanium TiO_2) n-type doping concentration on the parameters of solar cell has been studied. The donor concentration was varied from 10^{16} to 10^{21} cm^{-3}, by fixing ETL thickness to the value 30 nm. The simulation results are shown in Figure 3.18, where we observe with doping concentration increase, the Jsc and Voc are almost constant. Whereas, there is increase in fill factor (FF) from 82.24 to 82.78% and power conversion efficiency (PCE) from 24.89 to 25.05% with increasing doping concentration.

The increase in PCE is mainly due to the increase in FF, as the doping concentration increases. The conductivity value increase and the resistivity (R_s) decreases, which greatly affects the fill factor of the solar cell. Voc remains unchanged and independent of doping concentration in electron transport layer. Also, the open circuit voltage depends on the properties of the active layer.

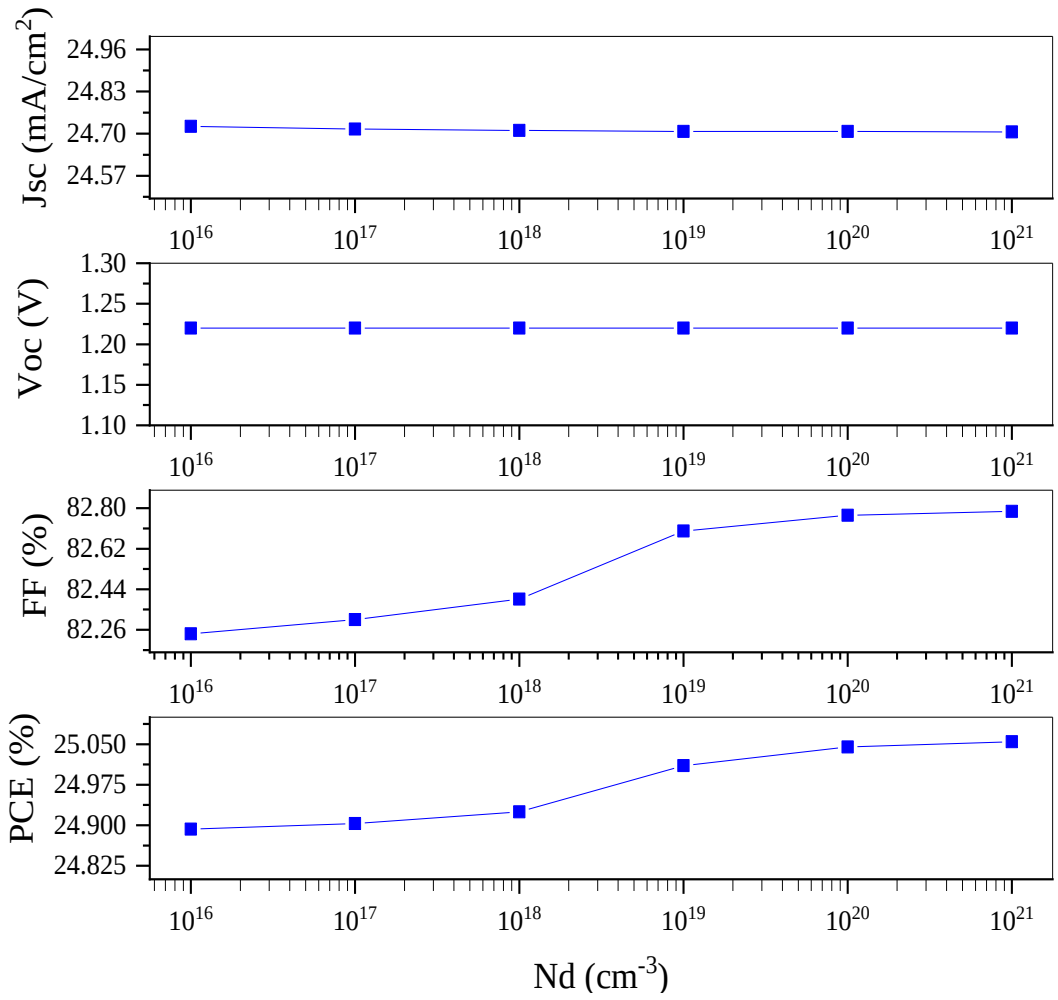

Figure 3.18: Influence of TiO_2 doping concentration on the solar cell performance.

3.3.3.3 Effect of TiO_2 defects on the performance of solar cell

The effect of defects concentration in the electron transport material (oxide titanium TiO_2) on the parameters of solar cell has been studied. Defects concentration was varied from 10^{14} to 10^{18} cm^{-3}, by fixing ETL (TiO_2) thickness to the value 30 nm. The density of defects concentration simulation results is shown in Figure 3.19. Although the increase of defects concentration, there is no change (almost constant) in open circuit voltage (Voc), short-circuit current (Jsc), power conversion efficiency (PCE) and fill factor (FF).

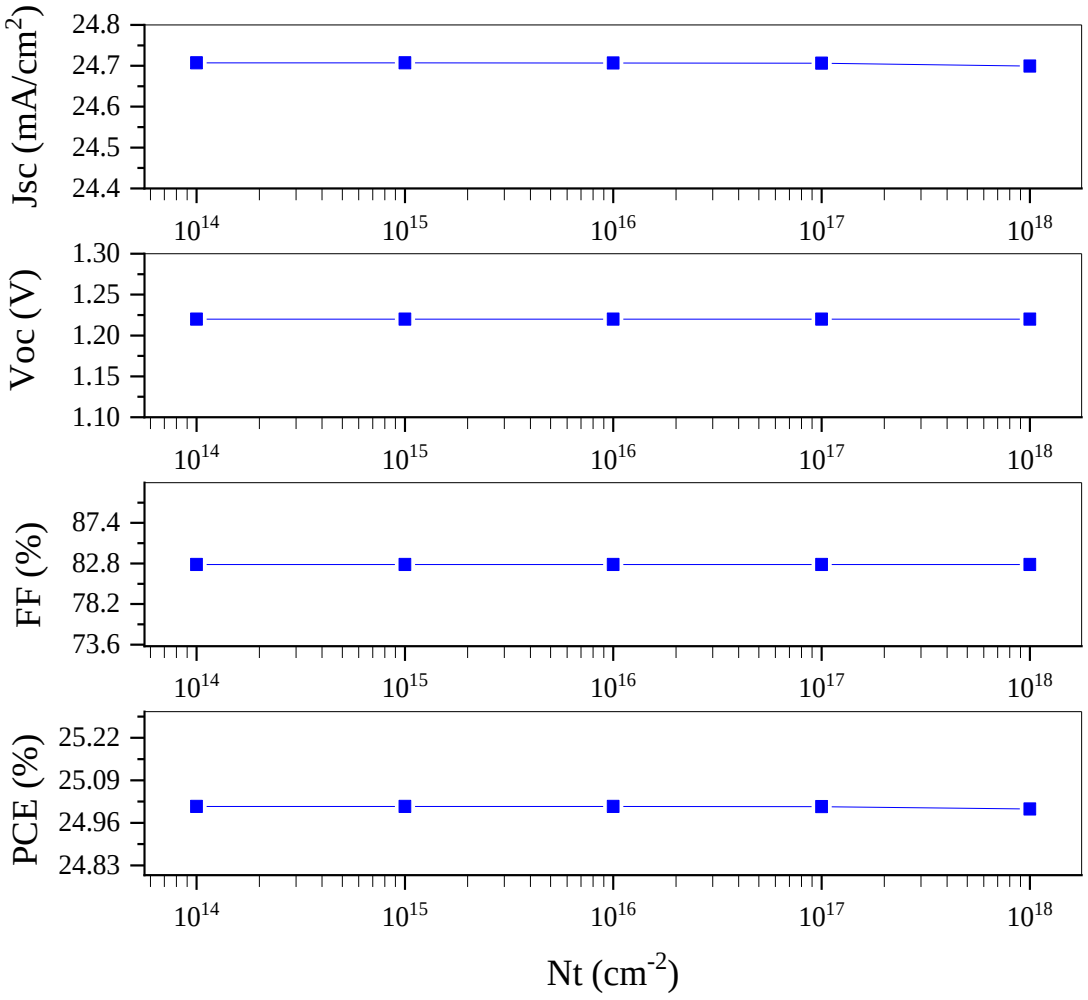

Figure 3.19: Influence of TiO_2 defect density on the solar cell performance.

3.3.3.4 Effect of interface trap density TiO_2/perovskite

Finally, the effect of interface TiO_2/Perovskite trap concentration on the parameters of solar cell has been studied. The interface trap concentration was varied from 10^8 to 10^{15} cm^{-2}, by fixing ETL

thickness at the value of 30 nm. The simulated J-V characteristics are shown in Figure 3.20, where we observe with increase trap concentration, the Voc decreases from 1.22 to 1.12 V.

The evaluated parameters of simulation results for increase interface trap concentration are shown in Figure 3.21. We observe that there is no effect on the parameters of solar cell for small defects concentrations. However, at high concentrations a decrease in the open circuit voltage Voc was observed starting from the value 10^{11} cm^{-2}, this is due to the presence of shunt resistance R_{sh}. The same effect can be observed on power conversion efficiency which decreases from 25.01 to 23.16 %. We see a similar effect in both Jsc and FF, where Jsc decreases but with small values from 24.70 to 24.58 mA/cm^2. While the Fill factor FF shows a strange behaviour, where it increases at concentrations from 10^{11} to 10^{12} cm^{-2} then it decreases like other parameters, this may be due to the combined effect of shunt resistance R_s and the ideality factor η.

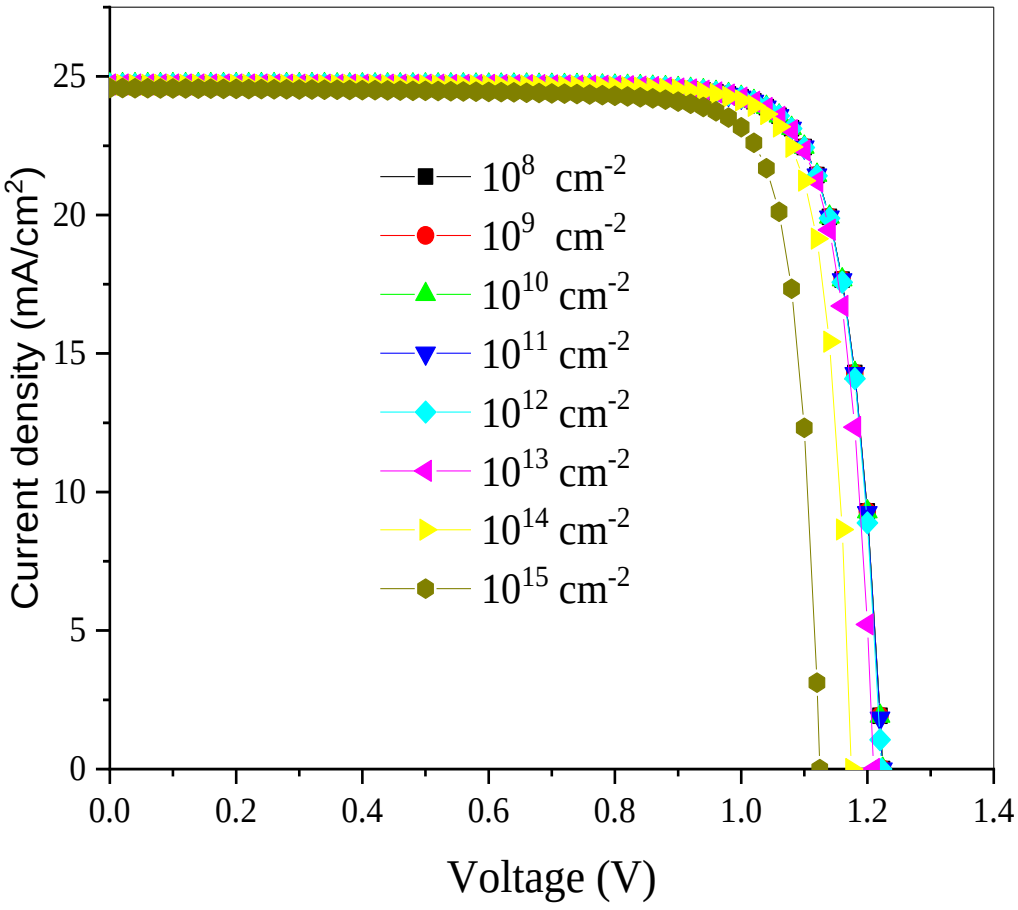

Figure 3.20: Effect of change interface traps density TiO_2/perovskite on the J-V characteristics.

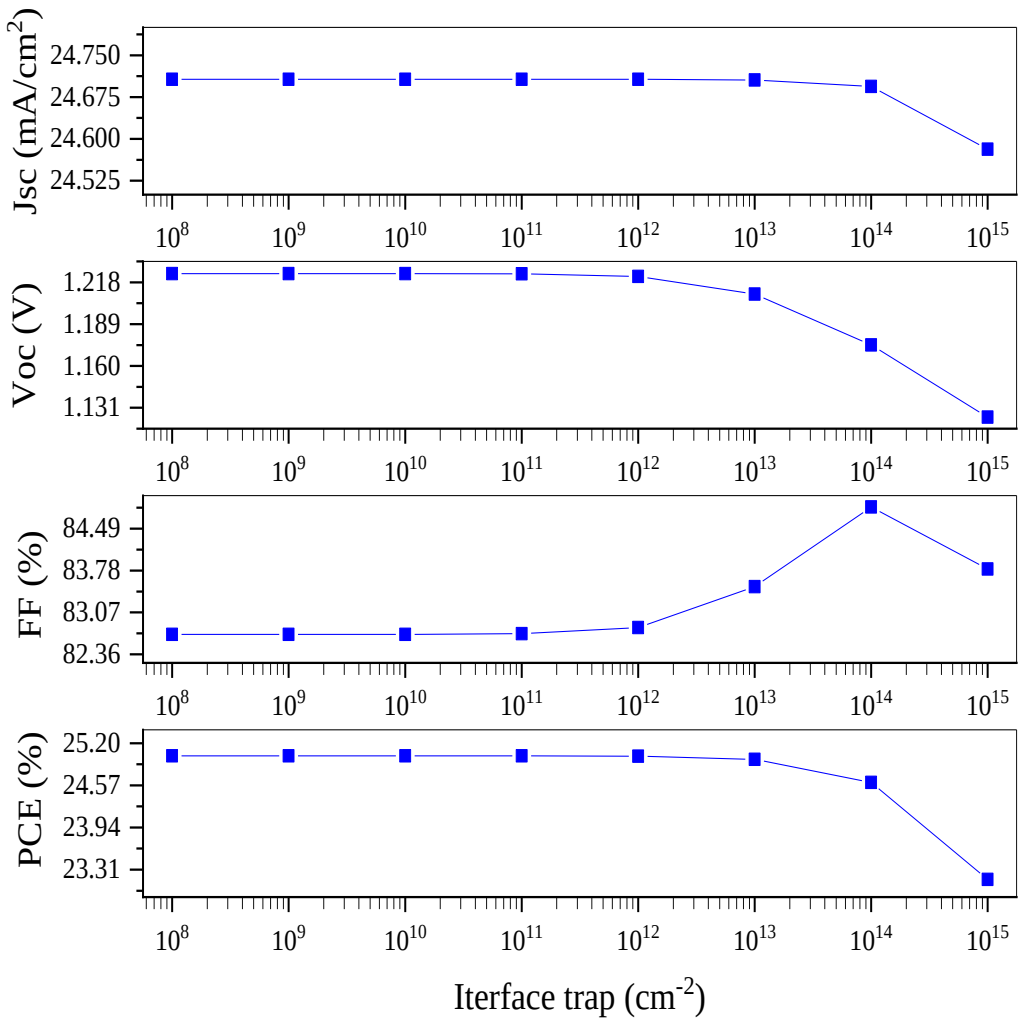

Figure 3.21: Influence of interface trap density on the solar cell performance.

3.3.4 Comparison

The simulation results of the electron transport layer using two different materials (zinc oxide, titanium dioxide) showed that a solar cell using titanium oxide is better than a solar cell based on zinc oxide despite its high mobility. And this is due to several reasons. The absorption coefficient can be one of these reasons, as shown in Figure 3.22, the absorption coefficient of zinc oxide is higher than that of titanium oxide. This mainly affects the extent of absorption of the active layer (perovskite). As most of the photons with short wavelengths are absorbed at the electron transfer layer (ZnO), which is located out of the active region, and this affects the number of the separated photo-generated carriers, and thus affects the performance of the solar cell.

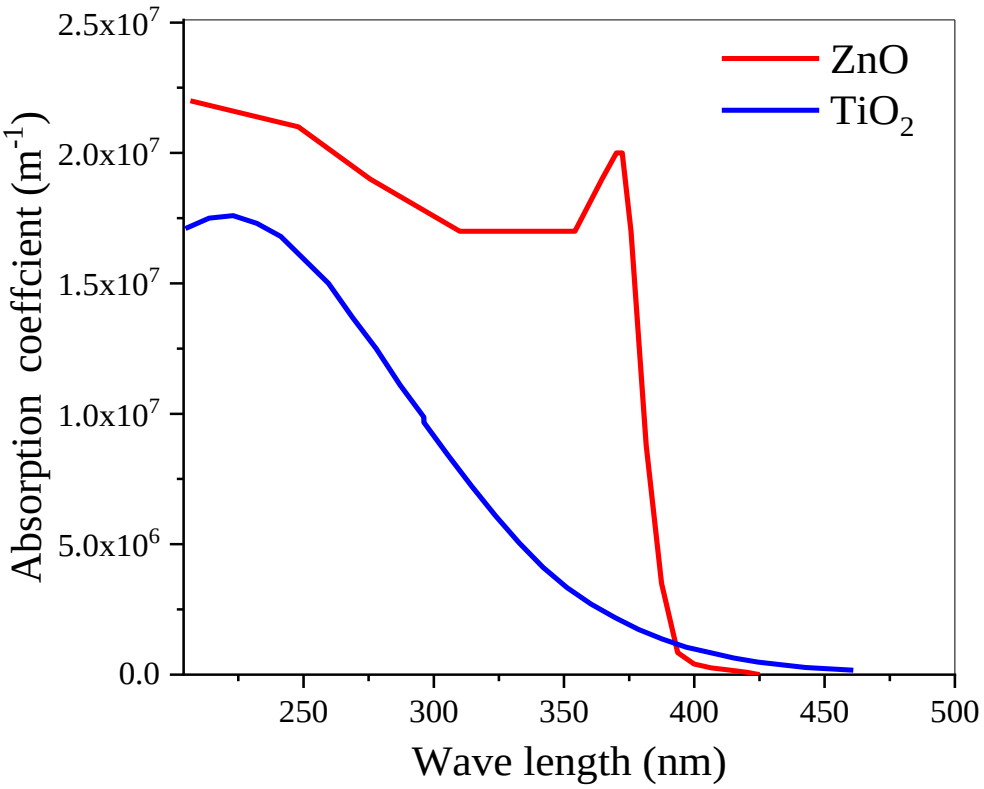

Figure 3.22: The absorption coefficient of ZnO and TiO_2 as a function of the vacuum wave length of light.

The difference in the performance of the solar cell can also be due to the difference in the electron affinity, or from another perspective, to the conduction band offset CBO. Where there is a preferable electron affinity, it can significantly affect the performance of the solar cell. When the electron affinity of ETL (χ ETL) is larger or smaller than absorber layer (χ absorber), the energy cliff with CBO (-) and the energy spike − CBO (+) formed respectively. In other words, if the conduction band (CB) of ETL is lower than that of the absorber, the energy Cliff CBO (−) is formed with no potential barrier for electrons at the ETL/absorber interface, and if CB of ETL is higher than that of the absorber layer, the energy spike-CBO (+) is formed at the ETL/absorber interface acting as barrier for electrons [132] . An advantage of the spike structure formed at the TiO2/absorber layer interface (see Figure 3.23), which can act as a barrier for photo-generated electron flow towards to the edge of ETL/absorber endows to enhance the photo-generation of free charge carriers. This will also suppress the recombination rate at the interface which is beneficial to increase the PV performance. Unlike the formation of cliff structure between ZnO/perovskite, the main recombination process is interface recombination, when the activation energy for carrier recombination (E_A) is less than the bandgap of the absorber layer. Also, the formation

of "cliff-type" band alignment will break the barrier for transfer of electron leading to decrease E_A and this affects directly the value of Voc, thus affecting the PCE of the solar cell.

The effect of CBO on V_{oc} can be illustrated according to the equation (3.10) and (3.11)

$$V_{oc} = \frac{E_a}{q} - \frac{nkT}{q} ln \frac{J_{00}}{J_{sc}} \tag{3.10}$$

$$E_A = E_g - CBO \tag{3.11}$$

V_{oc} is open circuit voltage, E_A is activation energy,n is diode ideality factor, K is Boltzmann constant, T is temperature, J_{00} is current pre factor and J_{sc} is short circuit current density.

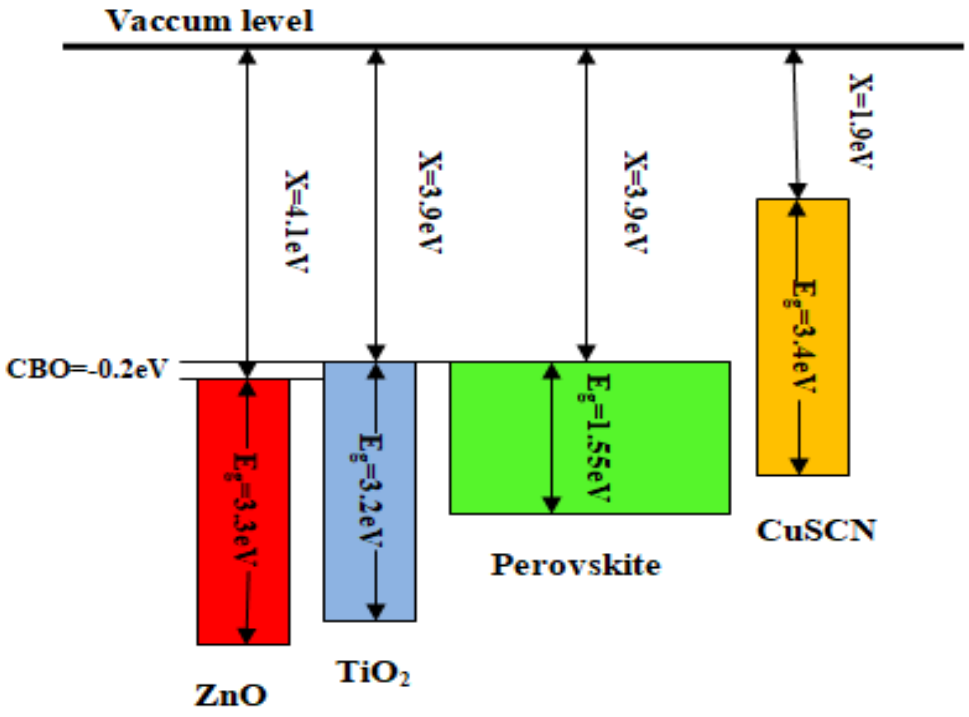

Figure 3.23: Energy levels diagram (relative to the vacuum level) of ZnO, TiO_2, perovskite and CuSCN films.

Conclusion

In this work, numerical simulation was carried out to estimate and analyze the parameters of different electron transport layer on performance of perovskite solar cells. Device modeling was performed on the dedicated simulation software "Solar Cell Capacitance Simulator" (SCAPS), to analyze the performance of a photovoltaic device with structure ETL/MAPbI3/CuSCN, the analysis was performed on two different materials (zinc oxide, titanium dioxide) with different physical parameters such as thickness, doping concentration, interface trap density ETL/perovskite and defect density of electron transport layer.

The zinc oxide-based solar cell as the electron transport layer gave an initial power conversion efficiency of 24.60%. It was found that the increase in both of thickness and defect density of the electron transport layer did not have a significant effect on the performance of the solar cell, where the power conversion efficiency decreased to 24.09% for the thickness and 24.56% for the defect density. Also, by increasing of n-type doping concentration the PCE increased to24.75%. Contrary to the above, it was found that the defect trap density ZnO/perovskite had the largest effect on the performance of the solar cell. Where the PCE decreased by (30%) of its initial value and it gave the following results: power conversion efficiency of 17.13%, fill factor of 69.65%, short circuit current density of 24.18 mA/cm^2 and open circuit voltage of 1.012 V at 1×10^{15} cm^2.
In contrast, the solar cell based on titanium dioxide as ETL gave an initial power conversion efficiency of 25.01%, higher than a solar cell based on zinc oxide. It also had the same behaviour as the previous solar cell when changing the thickness, defect density, and doping concentration. However, the interface trap density TiO_2/perovskite was not that much effect on the performance of the solar cell, as the PCE decreased by 8% of its initial value. And it achieved the following results: power conversion efficiency of 23.16%, fill factor of 83.80%, short circuit current density of 24.58 mA/cm^2 and open circuit voltage of 1.12V.

Perspectives

In this work an important role was revealed on the ETL, to determine their impact on perovskite solar cell behaviour and performance. In order to verify these results, an experimental study should be carried out. Explore other electron transport materials that may have a beneficial effect on perovskite solar cell.

References

[1] Swami R. Solar cell. International Journal of Scientific and Research Publications 2012;2:1-5.

[2] Kaushik A. Numerical Modeling of 3D Organic Solar Cells: San Diego State University; 2010.

[3] Nanduri SNR, Siddiki MK, Chaudhry GM, Alharthi YZ. Numerical simulation and performance optimization of perovskite solar cell. 2017 IEEE 44th Photovoltaic Specialist Conference (PVSC): IEEE; 2017. p. 1018-21.

[4] Smets AH, Jäger K, Isabella O, Swaaij RA, Zeman M. Solar energy: The physics and engineering of photovoltaic conversion, technologies and systems. UIT Cambridge; 2015.

[5] AZZOUZI G. Study of silicon solar cells performances using the impurity photovoltaic effect 2014.

[6] Faßl P. Exploration of Properties, Stability and Reproducibility of Perovskite Solar Cells 2019.

[7] Markvart T, Castañer L. Principles of solar cell operation. McEvoy's Handbook of Photovoltaics: Elsevier; 2018. p. 3-28.

[8] https://www.pveducation.org/pvcdrom/solar-cell-operation/quantum-efficiency.

[9] Ananda W. External quantum efficiency measurement of solar cell. 2017 15th International Conference on Quality in Research (QiR): International Symposium on Electrical and Computer Engineering: IEEE; 2017. p. 450-6.

[10] Lan C. Development of absorbing materials for perovskite solar cells: 九州工業大学; 2017.

[11] https://www.nrel.gov/pv/cell-efficiency.html.

[12] Mazer JA. Solar cells: an introduction to crystalline photovoltaic technology: Kluwer Academic Publishers Boston; 1996.

[13] Sharma S, Jain KK, Sharma A. Solar cells: in research and applications—a review. Materials Sciences and Applications 2015;6:1145.

[14] Green MA, Dunlop ED, Levi DH, Hohl-Ebinger J, Yoshita M, Ho-Baillie AW. Solar cell efficiency tables (version 54). Progress in photovoltaics: research and applications 2019;27:565-75.

[15] Shah A, Schade H, Vanecek M, Meier J, Vallat-Sauvain E, Wyrsch N, et al. Thin-film silicon solar cell technology. Progress in photovoltaics: Research and applications 2004;12:113-42.

[16] Zimmer T. 6. Photovoltaic cell types.

[17] Ramanujam J, Singh UP. Copper indium gallium selenide based solar cells–a review. Energy & Environmental Science 2017;10:1306-19.

[18] Gerngroß M-D, Reverey J. CIS/CIGS based Thin-film solar cells. Faculty of Engineering University of Kiel 2008.

[19] Woods KW. Solar Energy Conversion and Control Using Organic Photovoltaic Cells. 2013.

[20] Ganesan AA, Houtepen AJ, Crisp RW. Quantum dot solar cells: Small beginnings have large impacts. Applied Sciences 2018;8:1867.

[21] Luceño-Sánchez JA, Díez-Pascual AM, Peña Capilla R. Materials for photovoltaics: State of art and recent developments. International journal of molecular sciences 2019;20:976.

[22] Abdelmageed G, Jewell L, Hellier K, Seymour L, Luo B, Bridges F, et al. Mechanisms for light induced degradation in MAPbI3 perovskite thin films and solar cells. Applied Physics Letters 2016;109:233905.

[23] Jasim KE. Quantum dots solar cells. Solar Cells-New Approaches and Reviews 2015:303-31.

[24] Zulkifili ANB, Kento T, Daiki M, Fujiki A. The basic research on the dye-sensitized solar cells (DSSC). Journal of Clean Energy Technologies 2015;3:382-7.

[25] Toivola M. Dye-sensitized solar cells on alternative substrates. 2010.

[26] Park N-G. Perovskite solar cells: an emerging photovoltaic technology. Materials today 2015;18:65-72.

[27] Duan J, Xu H, Sha W, Zhao Y, Wang Y, Yang X, et al. Inorganic perovskite solar cells: an emerging member of the photovoltaic community. Journal of Materials Chemistry A 2019;7:21036-68.

[28] https://www.nature.com/articles/s41560-018-0323-9.

[29] Jena AK, Kulkarni A, Miyasaka T. Halide perovskite photovoltaics: background, status, and future prospects. Chemical reviews 2019;119:3036-103.

[30] https://www.energy.gov/articles/department-energy-announces-20-million-advance-perovskite-solar-technologies.

[31] Hussain I, Tran HP, Jaksik J, Moore J, Islam N, Uddin MJ. Functional materials, device architecture, and flexibility of perovskite solar cell. Emergent Materials 2018;1:133-54.

[32] Wei R. Modelling of perovskite solar cells: Queensland University of Technology; 2018.
[33] Nawaz A. Perovskite Solar Cells: Improved Active layer Morphology and Pore-filling in TiO2 Nano-Scaffolds. 2018.
[34] Stenberg J. Perovskite solar cells. UMEA UNIVERSITY: Master in Energy Engineering 2017.
[35] Kim H-S, Lee C-R, Im J-H, Lee K-B, Moehl T, Marchioro A, et al. Lead iodide perovskite sensitized all-solid-state submicron thin film mesoscopic solar cell with efficiency exceeding 9%. Scientific reports 2012;2:1-7.
[36] Hazeghi F, Ghorashi SMB. Simulation of perovskite solar cells by using CuSCN as an inorganic hole-transport material. Materials Research Express 2019;6:095527.
[37] Karimi E, Ghorashi SMB. The Effect of SnO 2 and ZnO on the Performance of Perovskite Solar Cells. Journal of Electronic Materials 2020;49:364-76.
[38] Bhoomanee C, Ruankhama P, Choopun S, Prathan A, Wongratanaphisan D. Effect of Al-doped ZnO for Electron Transporting Layer in Planar Perovskite solar cells. Materials Today: Proceedings 2019;17:1259-67.
[39] Djurišić AB, Leung YH. Optical properties of ZnO nanostructures. small 2006;2:944-61.
[40] Chouhan AS, Jasti NP, Avasthi S. The dual role of ozone-treated aluminum doped zinc oxide for CH3NH3PbI3 solar cells. Organic Electronics 2019;66:249-57.
[41] Azmi R, Hwang S, Yin W, Kim T-W, Ahn TK, Jang S-Y. High efficiency low-temperature processed perovskite solar cells integrated with alkali metal doped ZnO electron transport layers. ACS Energy Letters 2018;3:1241-6.
[42] Ali J, Li Y, Gao P, Hao T, Song J, Zhang Q, et al. Interfacial and structural modifications in perovskite solar cells. Nanoscale 2020;12:5719-45.
[43] Casas G, Cappelletti M, Cedola AP, Soucase BM, y Blancá EP. Analysis of the power conversion efficiency of perovskite solar cells with different materials as Hole-Transport Layer by numerical simulations. Superlattices and Microstructures 2017;107:136-43.
[44] Calio L, Kazim S, Graetzel M, Ahmad S. Hole-transport materials for perovskite solar cells. Angewandte Chemie International Edition 2016;55:14522-45.
[45] Tress W, Marinova N, Inganäs O, Nazeeruddin MK, Zakeeruddin SM, Graetzel M. The role of the hole-transport layer in perovskite solar cells-reducing recombination and increasing absorption. 2014 IEEE 40th Photovoltaic Specialist Conference (PVSC): IEEE; 2014. p. 1563-6.
[46] Zhu L, Xiao J, Shi J, Wang J, Lv S, Xu Y, et al. Efficient CH 3 NH 3 PbI 3 perovskite solar cells with 2TPA-n-DP hole-transporting layers. Nano Research 2015;8:1116-27.

[47] Bakr ZH, Wali Q, Fakharuddin A, Schmidt-Mende L, Brown TM, Jose R. Advances in hole transport materials engineering for stable and efficient perovskite solar cells. Nano Energy 2017;34:271-305.

[48] Zhang Y, Liu W, Tan F, Gu Y. The essential role of the poly (3-hexylthiophene) hole transport layer in perovskite solar cells. Journal of Power Sources 2015;274:1224-30.

[49] Chakrabarti T, Saha M, Khanda A, Sarkar SK. Modeling of Lead-Free CH 3 NH 3 SnI 3-Based Perovskite Solar Cell Using ZnO as ETL. Advances in Communication, Devices and Networking: Springer; 2018. p. 125-31.

[50] Mao G-P, Wang W, Shao S, Sun X-J, Chen S-A, Li M-H, et al. Research progress in electron transport layer in perovskite solar cells. Rare Metals 2018;37:95-106.

[51] Katz EA. Perovskite: Name Puzzle and German-Russian Odyssey of Discovery. Helvetica Chimica Acta 2020.

[52] Lew KC. Cathodoluminescence spectroscopy of organic-inorganic perovskites 2018.

[53] Wijeyasinghe N, Anthopoulos TD. Copper (I) thiocyanate (CuSCN) as a hole-transport material for large-area opto/electronics. Semiconductor Science and Technology 2015;30:104002.

[54] Ezealigo BN, Nwanya AC, Simo A, Bucher R, Osuji RU, Maaza M, et al. A study on solution deposited CuSCN thin films: Structural, electrochemical, optical properties. Arabian Journal of Chemistry 2020;13:346-56.

[55] Jaffe JE, Kaspar TC, Droubay TC, Varga T, Bowden ME, Exarhos GJ. Electronic and defect structures of CuSCN. The Journal of Physical Chemistry C 2010;114:9111-7.

[56] Tsetseris L. Copper thiocyanate: polytypes, defects, impurities, and surfaces. Journal of Physics: Condensed Matter 2016;28:295801.

[57] Ji W, Yue G-Q, Ke F-S, Wu S, Zhao H-B, Chen L-Y, et al. Electronic structures and optical properties of CuSCN with Cu vacancies. Journal of the Korean Physical Society 2012;60:1253-7.

[58] Murugadoss G, Thangamuthu R, Kumar SMS. Fabrication of CH3NH3PbI3 perovskite-based solar cells: Developing various new solvents for CuSCN hole transport material. Solar Energy Materials and Solar Cells 2017;164:56-62.

[59] Madhavan VE, Zimmermann I, Roldán-Carmona C, Grancini G, Buffiere M, Belaidi A, et al. Copper thiocyanate inorganic hole-transporting material for high-efficiency perovskite solar cells. ACS Energy Letters 2016;1:1112-7.

[60] Treat ND, Yaacobi-Gross N, Faber H, Perumal AK, Bradley DD, Stingelin N, et al. Copper thiocyanate: An attractive hole transport/extraction layer for use in organic photovoltaic cells. Applied Physics Letters 2015;107:66_1.

[61] Cheng Z, Lin J. Layered organic–inorganic hybrid perovskites: structure, optical properties, film preparation, patterning and templating engineering. CrystEngComm 2010;12:2646-62.

[62] Lang L, Yang J-H, Liu H-R, Xiang H, Gong X. First-principles study on the electronic and optical properties of cubic ABX3 halide perovskites. Physics Letters A 2014;378:290-3.

[63] Assirey EAR. Perovskite synthesis, properties and their related biochemical and industrial application. Saudi Pharmaceutical Journal 2019;27:817-29.

[64] Roy P, Sinha NK, Tiwari S, Khare A. A review on perovskite solar cells: Evolution of architecture, fabrication techniques, commercialization issues and status. Solar Energy 2020;198:665-88.

[65] Green MA, Ho-Baillie A, Snaith HJ. The emergence of perovskite solar cells. Nature photonics 2014;8:506-14.

[66] You P, Tang G, Yan F. Two-dimensional materials in perovskite solar cells. Materials today energy 2019;11:128-58.

[67] Elumalai NK, Uddin A. Hysteresis in organic-inorganic hybrid perovskite solar cells. Solar Energy Materials and Solar Cells 2016;157:476-509.

[68] Kojima A, Teshima K, Shirai Y, Miyasaka T. Organometal halide perovskites as visible-light sensitizers for photovoltaic cells. Journal of the American Chemical Society 2009;131:6050-1.

[69] Marronnier A. Anharmonicity and Instabilities in Halide Perovskites for Last Generation Solar Cells 2018.

[70] Domanski K. The Quest for Stability of Perovskite Solar Cells: Understanding Degradation, Improving Lifetimes and Towards Experimental Standards: Ecole Polytechnique Fédérale de Lausanne; 2018.

[71] Christians JA, Fung RC, Kamat PV. An inorganic hole conductor for organo-lead halide perovskite solar cells. Improved hole conductivity with copper iodide. Journal of the American Chemical Society 2014;136:758-64.

[72] Boix PP, Nonomura K, Mathews N, Mhaisalkar SG. Current progress and future perspectives for organic/inorganic perovskite solar cells. Materials today 2014;17:16-23.

[73] Baikie T, Fang Y, Kadro JM, Schreyer M, Wei F, Mhaisalkar SG, et al. Synthesis and crystal chemistry of the hybrid perovskite (CH 3 NH 3) PbI 3 for solid-state sensitised solar cell applications. Journal of Materials Chemistry A 2013;1:5628-41.

[74] Hossain S. Performance and stability of perovskite solar cells 2018.

[75] Hossain S. Performance and stability of perovskite solar cells 2018.

[76] Xiao Z, Dong Q, Bi C, Shao Y, Yuan Y, Huang J. Solvent annealing of perovskite-induced crystal growth for photovoltaic-device efficiency enhancement. Advanced Materials 2014;26:6503-9.

[77] Xing G, Mathews N, Sun S, Lim SS, Lam YM, Grätzel M, et al. Long-range balanced electron-and hole-transport lengths in organic-inorganic CH3NH3PbI3. Science 2013;342:344-7.

[78] Zhou J, Tang FL, Xue HT, Si FJ. Orientation Effects of CH3NH3+ on CH3NH3PbI3 Stability and Photoelectric Properties. Materials Science Forum: Trans Tech Publ; 2016. p. 245-52.

[79] Noh JH, Im SH, Heo JH, Mandal TN, Seok SI. Chemical management for colorful, efficient, and stable inorganic–organic hybrid nanostructured solar cells. Nano letters 2013;13:1764-9.

[80] Shi Z, Jayatissa AH. Perovskites-based solar cells: A review of recent progress, materials and processing methods. Materials 2018;11:729.

[81] Yang D, Yang R, Priya S, Liu S. Recent advances in flexible perovskite solar cells: fabrication and applications. Angewandte Chemie International Edition 2019;58:4466-83.

[82] SALA G. Hybrid perovskite-based solar cells: photoactive layer morphology optimization towards printed devices. 2016.

[83] Holliman PJ, Jones EW, Connell A, Ghosh S, Furnell L, Hobbs RJ. Solvent issues during processing and device lifetime for perovskite solar cells. Materials Research Innovations 2015;19:508-11.

[84] Seo Y-H, Kim E-C, Cho S-P, Kim S-S, Na S-I. Hysteresis data of planar perovskite solar cells fabricated with different solvents. Data in brief 2018;16:418-22.

[85] Ko H-S, Lee J-W, Park N-G. 15.76% efficiency perovskite solar cells prepared under high relative humidity: importance of PbI 2 morphology in two-step deposition of CH 3 NH 3 PbI 3. Journal of Materials Chemistry A 2015;3:8808-15.

[86] Chen Q, Zhou H, Hong Z, Luo S, Duan H-S, Wang H-H, et al. Planar heterojunction perovskite solar cells via vapor-assisted solution process. Journal of the American Chemical Society 2014;136:622-5.

[87] Liu M, Johnston MB, Snaith HJ. Efficient planar heterojunction perovskite solar cells by vapour deposition. Nature 2013;501:395-8.

[88] Cui J, Yuan H, Li J, Xu X, Shen Y, Lin H, et al. Recent progress in efficient hybrid lead halide perovskite solar cells. Science and technology of advanced materials 2015;16:036004.

[89] Anwar F, Mahbub R, Satter SS, Ullah SM. Effect of different HTM layers and electrical parameters on ZnO nanorod-based lead-free perovskite solar cell for high-efficiency performance. International Journal of Photoenergy;2017.

[90] Aseena S, Abraham N, Babu VS. A Novel Perovskite Solar Cell with ZnO-Cu 2 O as Electron Transport Material-Hole Transport Material. 2019 TEQIP III Sponsored International Conference on Microwave Integrated Circuits, Photonics and Wireless Networks (IMICPW): IEEE; 2019. p. 131-5.

[91] Zhang P, Wu J, Zhang T, Wang Y, Liu D, Chen H, et al. Perovskite solar cells with ZnO electron-transporting materials. Advanced Materials 2018;30:1703737.

[92] Eshaghi A, Hajkarimi M. Optical and electrical properties of aluminum zinc oxide (AZO) nanostructured thin film deposited on polycarbonate substrate. Optik 2014;125:5746-9.

[93] Baltakesmez A, Biber M, Tüzemen S. Inverted planar perovskite solar cells based on Al doped ZnO substrate. Journal of radiation research and applied sciences 2018;11:124-9.

[94] Kim M-S, Yim K-G, Son J-S, Leem J-Y. Effects of Al concentration on structural and optical properties of Al-doped ZnO thin films. Bulletin of the Korean Chemical Society 2012;33:1235-41.

[95] Sharma S, Tran A, Nalamasu O, Dutta P. Spin-coated ZnO thin films using ZnO nano-colloid. Journal of electronic materials 2006;35:1237-40.

[96] Luo J, Wang Y, Zhang Q. Progress in perovskite solar cells based on ZnO nanostructures. Solar Energy 2018;163:289-306.

[97] Bouaichi F. Deposition and analysis of Zinc Oxide thin films elaborated using spray pyrolysis for photovoltaic applications: University Mohamed Khider of Biskra; 2019.

[98] Gao Z, Banerjee P. Atomic layer deposition of doped ZnO films. Journal of Vacuum Science & Technology A: Vacuum, Surfaces, and Films 2019;37:050802.

[99] Ellmer K, Mientus R. Carrier transport in polycrystalline transparent conductive oxides: A comparative study of zinc oxide and indium oxide. Thin solid films 2008;516:4620-7.

[100] Thakur UK, Kisslinger R, Shankar K. One-dimensional electron transport layers for perovskite solar cells. Nanomaterials 2017;7:95.

[101] Mahmood K, Sarwar S, Mehran MT. Current status of electron transport layers in perovskite solar cells: materials and properties. Rsc Advances 2017;7:17044-62.

[102] Khan AF, Mehmood M, Durrani S, Ali M, Rahim N. Structural and optoelectronic properties of nanostructured TiO2 thin films with annealing. Materials Science in Semiconductor Processing 2015;29:161-9.

[103] Lu H, Ma Y, Gu B, Tian W, Li L. Identifying the optimum thickness of electron transport layers for highly efficient perovskite planar solar cells. Journal of Materials Chemistry A 2015;3:16445-52.

[104] Mohammed NM, Bashiri R, Sufian S, Kait CF, Majidai S. One-dimensional titanium dioxide and its application for photovoltaic devices. Titanium Dioxide: Material for a Sustainable Environment 2018:367.

[105] Li B, Li Y, Zheng C, Gao D, Huang W. Advancements in the stability of perovskite solar cells: degradation mechanisms and improvement approaches. RSC advances 2016;6:38079-91.

[106] Zhao X, Park N-G. Stability issues on perovskite solar cells. Photonics: Multidisciplinary Digital Publishing Institute; 2015. p. 1139-51.

[107] Roknuzzaman M, Zhang C, Ostrikov KK, Du A, Wang H, Wang L, et al. Electronic and optical properties of lead-free hybrid double perovskites for photovoltaic and optoelectronic applications. Scientific reports 2019;9:1-7.

[108] Senocrate A, Kim GY, Grätzel M, Maier J. Thermochemical stability of hybrid halide perovskites. ACS Energy Letters 2019;4:2859-70.

[109] Boyd CC, Cheacharoen R, Leijtens T, McGehee MD. Understanding degradation mechanisms and improving stability of perovskite photovoltaics. Chemical reviews 2018;119:3418-51.

[110] Mesquita I, Andrade L, Mendes A. Effect of relative humidity during the preparation of perovskite solar cells: Performance and stability. Solar Energy 2020;199:474-83.

[111] Noh MFM, Arzaee NA, Mumthas INN, Mohamed NA, Nasir SNFM, Safaei J, et al. High-humidity processed perovskite solar cells. Journal of Materials Chemistry A 2020;8:10481-518.

[112] Ciccioli A, Latini A. Thermodynamics and the intrinsic stability of lead halide perovskites CH3NH3PbX3. The journal of physical chemistry letters 2018;9:3756-65.

[113] Leijtens T, Bush K, Cheacharoen R, Beal R, Bowring A, McGehee MD. Towards enabling stable lead halide perovskite solar cells; interplay between structural, environmental, and thermal stability. Journal of Materials Chemistry A 2017;5:11483-500.

[114] Kim N-K, Min YH, Noh S, Cho E, Jeong G, Joo M, et al. Investigation of thermally induced degradation in CH 3 NH 3 PbI 3 perovskite solar cells using in-situ synchrotron radiation analysis. Scientific reports 2017;7:1-9.

[115] Immonen J. Promises and Challenges of Perovskite Solar Cells in Portable Applications 2017.

[116] Rahman NU, Khan WU, Li W, Khan S, Khan J, Zheng S, et al. Simultaneous enhancement in performance and UV-light stability of organic–inorganic perovskite solar cells using a samarium-based down conversion material. Journal of Materials Chemistry A 2019;7:322-9.

[117] Domanski K, Correa-Baena J-P, Mine N, Nazeeruddin MK, Abate A, Saliba M, et al. Not all that glitters is gold: metal-migration-induced degradation in perovskite solar cells. ACS nano 2016;10:6306-14.

[118] Tress W. Metal Halide Perovskites as Mixed Electronic–Ionic Conductors: Challenges and Opportunities□ From Hysteresis to Memristivity. The journal of physical chemistry letters 2017;8:3106-14.

[119] Calado P, Telford AM, Bryant D, Li X, Nelson J, O'Regan BC, et al. Evidence for ion migration in hybrid perovskite solar cells with minimal hysteresis. Nature communications 2016;7:1-10.

[120] Li C, Tscheuschner S, Paulus F, Hopkinson PE, Kießling J, Köhler A, et al. Iodine migration and its effect on hysteresis in perovskite solar cells. Advanced Materials 2016;28:2446-54.

[121] van Reenen S, Kemerink M, Snaith HJ. Modeling anomalous hysteresis in perovskite solar cells. The journal of physical chemistry letters 2015;6:3808-14.

[122] Evasari ER. Electrical Modeling of Perovskite Solar Cells. 2018.

[123] Kour N, Mehra R. Recent Advances in Photovoltaic technology based on perovskite solar cell-A review. International Research Journal of Engineering and Technology (IRJET) 2017;4:2395-0056.

[124] Agobi AU, Hitler L, Ahmed S, Funmilayoe OO, Zafar S-U, Hamzatf AT, et al. Perovskite photovoltaic nanostructured materials: device architectural design, challenges and recent progress. Asian Journal of Green Chemistry 2019;3:153-68.

[125] Babayigit A, Ethirajan A, Muller M, Conings B. Toxicity of organometal halide perovskite solar cells. Nature materials 2016;15:247.

[126] Jain SM, Edvinsson T, Durrant JR. Green fabrication of stable lead-free bismuth based perovskite solar cells using a non-toxic solvent. Communications Chemistry 2019;2:1-7.

[127] Khattak YH. Modeling of high power conversion efficiency thin film solar cells 2019.

[128] Burgelman M, Decock K, Niemegeers A, Verschraegen J, Degrave S. SCAPS manual. February; 2016.

[129] Husainat A, Ali W, Cofie P, Attia J, Fuller J. Simulation and Analysis of Methylammonium Lead Iodide (CH3NH3PbI3) Perovskite Solar Cell with Au Contact Using SCAPS 1D Simulator. American Journal of Optics and Photonics 2019;7:33.

[130] MaríSoucase B, Pradas IG, Adhikari KR. Numerical Simulations on Perovskite Photovoltaic Devices. Perovskite Materials: Synthesis, Characterisation, Properties, and Applications 2016:445.

[131] Amu TL. Performance Optimization of tin halide Perovskite solar cells via Numerical Simulation 2014.

[132] Raoui Y, Ez-Zahraouy H, Kazim S, Ahmad S. Energy level engineering of charge selective contact and halide perovskite by modulating band offset: Mechanistic insights. 2020.